Available online at www.sciencedirect.com
ScienceDirect
Geochimica et Cosmochimica Acta 74 (2010) 2450–2472
Geochimica et Cosmochimica Acta
www.elsevier.com/locate/gca

Detrital zircon evidence for Hf isotopic evolution of granitoid crust and continental growth

Tsuyoshi Iizuka *, Tsuyoshi Komiya, Shuji Rino, Shigenori Maruyama, Takafumi Hirata [1]

Department of Earth and Planetary Sciences, Tokyo Institute of Technology, O-okayama 2-12-1, Meguro-ku, Tokyo 152-8551, Japan

Received 4 June 2009; accepted in revised form 21 January 2010; available online 28 January 2010

Abstract

We have determined U–Pb ages, trace element abundances and Hf isotopic compositions of approximately 1000 detrital zircon grains from the Mississippi, Congo, Yangtze and Amazon Rivers. The U–Pb isotopic data reveal the lack of >3.3 Ga zircons in the river sands, and distinct peaks at 2.7–2.5, 2.2–1.9, 1.7–1.6, 1.2–1.0, 0.9–0.4, and <0.3 Ga in the accumulated age distribution. These peaks correspond well with the timing of supercontinent assembly. The Hf isotopic data indicate that many zircons, even those having Archean U–Pb ages, crystallized from magmas involving an older crustal component, suggesting that granitoid magmatism has been the primary agent of differentiation of the continental crust since the Archean era. We calculated Hf isotopic model ages for the zircons to estimate the mean mantle-extraction ages of their source materials. The oldest zircon Hf model ages of about 3.7 Ga for the river sands suggest that some crust generation had taken place by 3.7 Ga, and that it was subsequently reworked into <3.3 Ga granitoid continental crust. The accumulated model age distribution shows peaks at 3.3–3.0, 2.9–2.4, and 2.0–0.9 Ga.

The striking attribute of our new data set is the non-uniformitarian secular change in Hf isotopes of granitoid crusts; Hf isotopic compositions of granitoid crusts deviate from the mantle evolution line from about 3.3 to 2.0 Ga, the deviation declines between 2.0 and 1.3 Ga and again increases afterwards. Consideration of mantle-crust mixing models for granitoid genesis suggests that the noted isotopic trends are best explained if the rate of crust generation globally increased in two stages at around (or before) 3.3 and 1.3 Ga, whereas crustal differentiation was important in the evolution of the continental crust at 2.3–2.2 Ga and after 0.6 Ga. Reconciling the isotopic secular change in granitoid crust with that in sedimentary rocks suggests that sedimentary recycling has essentially taken place in continental settings rather than active margin settings and that the sedimentary mass significantly grew through addition of first-cycle sediments from young igneous basements, until after ~1.3 Ga when sedimentary recycling became the dominant feature of sedimentary evolution. These findings, coupled with the lack of zircons older than 3.3 Ga in river sands, imply the emergence of large-scale continents at about 3.3 Ga with further rapid growth at around 1.3 Ga. This resulted in the major growth of the sedimentary mass between 3.3 and 1.3 Ga and the predominance of its cannibalistic recycling later.

1. INTRODUCTION

One of the Earth's unique features among the known terrestrial planets is the presence of a chemically evolved and voluminous crust – the continental crust (Campbell and Taylor, 1983). It is generally accepted that present-day continental crust has an andesitic bulk composition and is vertically stratified in terms of lithological and

* Corresponding author. Present address: Research School of Earth Sciences, Australian National University, Canberra, ACT 0200, Australia. Fax: +61 2 6125 0941.
E-mail address: tsuyoshi.iizuka@anu.edu.au (T. Iizuka).
[1] Present address: Laboratory for Planetary Sciences, Kyoto University, Kyoto 606-8502, Japan.

0016-7037/$ - see front matter © 2010 Elsevier Ltd. All rights reserved.
doi:10.1016/j.gca.2010.01.023

chemical compositions – from lower portions dominated by mafic rocks to upper portions dominated by granitoids (Taylor and Mclennan, 1985; Christensen and Mooney, 1995; Rudnick and Fountain, 1995; Wedepohl, 1995; Gao et al., 1998). Yet there is considerable debate as to when and how it has evolved to its present form (e.g., Rudnick, 1995; Albarède, 1998; Tatsumi, 2000; Hawkesworth and Kemp, 2006; Rollinson, 2008). Of the two contrasting models of continental growth, the first is that the volume of continental crust has increased progressively with time (Hurley and Rand, 1969; Moorbath, 1978), as manifested by the present areal extent of continental crust of different ages (Veizer and Jansen, 1985). The second argues that a near-present mass of continents formed within the first billion years of Earth history with little subsequent growth (no-growth model), implying that the present age distribution is the result of the recycling of older continental crust (Fyfe, 1978; Armstrong, 1981; Bowring and Housh, 1995; Harrison, 2009). More recently, the striking peaks in radiogenic isotope model ages of granitoids and sediments have been recognized (Nelson and DePaolo, 1985; Patchett and Arndt, 1986; McCulloch and Bennett, 1994; Jahn, 2004; Kemp et al., 2006; Wang et al., 2009; Yang et al., 2009). This has led to a third model in which the continental crust has grown throughout geological time with pulses at higher rates, possibly in response to major mantle instabilities such as superplumes (Hill, 1993; Stein and Hofmann, 1994; Stein and Golstein, 1996; Condie, 1998; Albarède, 1998; Davies, 2008). The challenge in deciphering the evolutionary history lies with better understanding the role of granitoid genesis in continental crust development.

Granitoid genesis by melting of pre-existing continental crust has been considered to be the principal agent of crustal differentiation to shape the compositional structure of the continental crust (e.g., Wyllie, 1984; Taylor and McLennan, 1985). Granitoid magmas formed by intra-crustal melting inherit the radiogenic isotopic compositions of the reworked crust (e.g., DePaolo and Wasserburg, 1976). By contrast, newly generated continental crust has radiogenic isotopic compositions indistinguishable from those of its mantle source (e.g., DePaolo, 1981). Because crustal generation processes transfer heat and (in a subduction setting) volatiles into continental crust, crustal generation is likely accompanied by crustal differentiation. This results in the genesis of granitoid magmas involving a juvenile component and a reworked crustal component (e.g., Voshage et al., 1990; Petford and Gallagher, 2001; Annen et al., 2006; Kemp et al., 2007; Jagoutz et al., 2009). Therefore, radiogenic isotopic evolution of granitoid crust potentially records the generation and differentiation history of the continental crust (Allègre and Ben Othman, 1980), leading to more robust models for the continental growth. In addition, if the temporal isotopic evolution of granitoid crust can be established, it can be used to infer the growth and recycling of the sedimentary mass by reconciling it with the isotopic secular change in sedimentary rocks.

Previous attempts at constraining the radiogenic isotopic evolution of granitoid crust (e.g., Moorbath, 1978; Allègre and Ben Othman, 1980; Patchett et al., 1981) have suggested that the isotopic compositions generally deviate from the mantle evolution line through time, with an implication that this reflects quasi-continuous continental growth. However, these studies utilized only a limited number of granitoid samples and considering that granitoid crust is significantly diverse and heterogeneous, their interpretation is speculative. Furthermore, because a significant part of granitoid crust is covered by sediments and therefore inaccessible to *in situ* sampling and measurements at present, it may be difficult to arrive at a reliable secular trend based solely on the exposed geology.

These problems can be largely circumvented by using detrital zircons from large rivers. Large rivers erode exposed continental crust over an extensive area, and most eroded materials have experienced sediment–sediment recycling (sedimentary recycling) (Veizer and Jansen, 1979, 1985; Goldstein et al., 1984; Campbell et al., 2005) as well as several current erosion cycles before transfer to river mouths (Dosseto et al., 2006). Prolonged sedimentary recycling results in efficient mixing of sediments derived from various source rocks, including the parts of granitoid crust that are currently inaccessible. Zircon, which is ubiquitous as an accessory mineral in granitoids, can be precisely dated by U–Pb isotopes, and is well suited for Hf isotopic studies (e.g., Patchett et al., 1981; Amelin et al., 2000; Griffin et al., 2000). Moreover, due to its robustness zircon can retain primary isotopic information through sedimentary and metamorphic processes. Accordingly, an integration of U–Pb and Hf isotopic data of detrital zircons from large rivers may be the best way to evaluate secular changes of radiogenic isotopes in granitoids on a continental scale (Bodet and Schärer, 2000). So far, we have accumulated U–Pb, Hf isotopic and trace element data for approximately 1000 zircon grains from the Mississippi (Iizuka et al., 2005), Congo, Yangtze, and Amazon Rivers, that reveal significant Hf isotopic secular trends. Here we use the results to evaluate the evolution of the sedimentary system and continental growth history.

2. SAMPLES AND METHODS

The sand samples were collected at or near the mouths of the Mississippi (MP1), Amazon (AMZ8), Yangtze (YZ1), and Congo (CNG2) Rivers. These include the largest three rivers on Earth according to the size of their drainage areas (Milliman and Syvitski, 1992) (Table 1). Zircons were concentrated from the sand samples using magnetic separation and heavy-liquid techniques. The aliquots of zircon concentrates were used by Rino et al. (2004, 2008) for zircon U–Pb dating. In this study, zircon grains were newly prepared for a comprehensive U–Pb, trace element and Lu–Hf analytical work. The grains were mounted in epoxy and were polished to reveal their interiors. Caution was taken to minimize preferential selection of zircon grains during mounting. Before isotopic analyses, the zircons were imaged using cathodoluminesence (CL) imaging to reveal any internal structure. CL images were obtained using a JEOL JSM-5310 scanning electron microprobe combined with an Oxford CL system at the Tokyo Institute of Technology. For analyses, we selected oscillatory- or sector-zoned zircons that were likely to preserve the magmatic

Table 1
Summary of the samples used in this study.

Sample	River	Sample locality	N of analyzed grains	Drainage area† ($\times 10^6$ km^2)	Sediment load† ($\times 10^6$ t/yr)
MP1	Mississippi	30°29′40″N, 91°11′33″W	416	3.3	400
CNG2	Congo	40°17′08″S, 15°27′29″E	213	3.8	43
YZ1	Yangtze	Nanjing Danjao Park	158	1.9	480
AMZ8	Amazon	Santana Island	230	6.1	1200

† Data are from Milliman and Syvitski (1992).

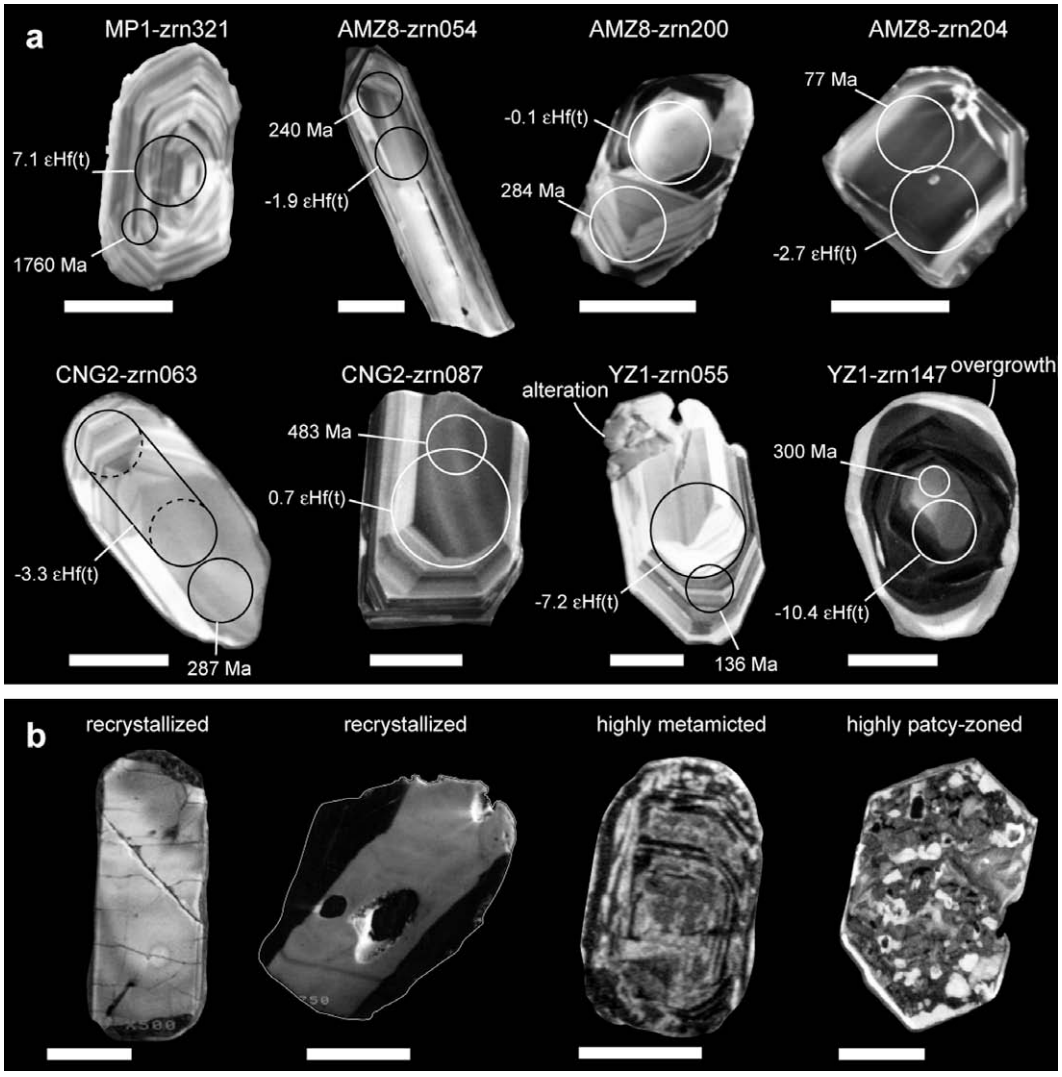

Fig. 1. Representative cathodoluminescence images for (a) igneous zircons (oscillatory- or sector-zoned) and (b) metamorphic or altered zircons (little-, no-, or highly patchy-zoned) in the river sands. Laser ablation sites for U–Pb isotopic-trace element and Hf isotopic analyses are shown, together with U–Pb ages and εHf(t) values. Scale bars are all 50 μm.

chemistry (Fig. 1a); we avoided little/no-zoned and highly patch-zoned zircons (Fig. 1b), that have been interpreted as metamorphic or alteration in origin (Hoskin and Black, 2000; Rubatto, 2002).

Determinations of U–Pb age and trace element abundances (La, Ce, Pr, Sm, Eu, Gd, Yb, and Hf for zircons from MP1 and additional Y, Nb, Ho for zircons from AMZ8, YZ1 and CNG2) were concurrently performed on a laser ablation-inductively coupled plasma mass spectrometer (LA-ICPMS) at the Tokyo Institute of Technology. The ICPMS instrument used in this study was a ThermoElemental VG PlasmaQuad 2 quadrupole-based ICPMS equipped with a S-option interface and chicane ion lens (Iizuka and Hirata, 2004). The laser ablation system was a MicroLas production (Gottingen, Germany) GeoLas 200CQ which utilizes an ArF excimer laser as a 193 nm deep ultraviolet light source. Helium gas was flushed into the ablation cell, minimizing aerosol deposition around

the ablation pit and improving transport efficiency. To improve the stability of the signals, a gas expansion chamber was inserted between the ablation cell and the ICP ion source (Tunheng and Hirata, 2004).

The data were obtained from two different sizes of ablation craters (16 and 32 μm) with the integration time of 20 s, a laser repetition rate of 4–6 Hz, and emission power of 4–5 mJ. Samples were analyzed in runs of ~28 analyses which included ~12 unknown sample analyses, bracketed by 4 analyses of the SL13 or 91500 zircon standards and four analyses of NIST 610 SRM. The instrumental mass bias and ablation-related fractionation were corrected using the results of the bracketing standard analyses. Normalization for $^{206}Pb/^{238}U$ was made against the SL13 (0.09281: Roddick and van Breemen, 1994) or 91500 standard zircons (0.17917: Wiedenbeck et al., 1995), and for $^{207}Pb/^{206}Pb$ against NIST SRM 610 (0.9096: Hirata and Nesbitt, 1995; Iizuka and Hirata, 2004), respectively. Common Pb was corrected using ^{204}Pb. The isobaric interference of ^{204}Hg on ^{204}Pb was corrected by monitoring ^{202}Hg. To reduce the isobaric interference of ^{204}Hg, a Hg-trap device using an activated charcoal filter was applied to the Ar make-up gas before mixing with He carrier gas (Hirata et al., 2005). No common Pb correction has been applied to analyses where the corrected ratio is within analytical uncertainty of the uncorrected ratio. Analytical uncertainties combine the counting statistics and the reproducibility of standard analyses, added in quadrature. The U–Pb age in the following discussion represents the $^{207}Pb/^{206}Pb$ age for zircons older than 1.0 Ga, and the $^{206}Pb/^{238}U$ age for younger zircons. For the trace element analyses, the peaks ^{89}Y, ^{93}Nb, ^{139}La, ^{140}Ce, ^{141}Pr, ^{147}Sm, ^{151}Eu, ^{157}Gd, ^{165}Ho, ^{172}Yb, ^{179}Hf were measured, and the data were normalized against NIST SRM 610.

The Lu–Hf isotopic analyses were performed using the ArF excimer laser ablation system attached to a Nu Plasma 500 MC-ICPMS at the Tokyo Institute of Technology. The Nu Plasma 500 MC-ICPMS contains 12 Faraday collectors. The dispersion of the spectrometer is adjusted by using a pair of quadrupole lenses that act as zoom lenses, focusing the ion beams into the Faraday collectors. The lenses were set to detect ^{171}Yb, ^{173}Yb, ^{175}Lu, $^{176}(Hf + Yb + Lu)$, ^{177}Hf, ^{178}Hf, ^{179}Hf and (^{180}Hf) simultaneously. Helium gas was used for flushing the ablation pit. Furthermore, 4 ml/min N_2 was mixed into the Ar sample carrier gas to enhance the signal sensitivity. Analyses were carried out with beam diameters of 35 or 63 μm, 6–15 Hz repetition rates, and ~60 sec ablation times. To correlate Lu–Hf isotopic data with the U–Pb age and trace element abundances properly, the laser ablation site for Lu–Hf isotopic analysis was placed within similar internal domains and close to the original pit for U–Pb isotopic and trace element analysis (Fig. 1a). Line-scan analysis, rather than spot analysis, was utilized for some grains having neither multiple growth nor altered domains (e.g., CNG2-zrn063 and c.f., YZ1-zrn055 and 147; Fig. 1a), as the technique produces relatively stable signal intensity profile. All Lu–Hf isotopic analyses were carried out using a time-resolved analytical procedure, in which signal intensities for each mass and isotope ratios including initial $^{176}Hf/^{177}Hf$ are displayed as a function of time during the analysis. This procedure allows one to evaluate the depth profile isotopic homogeneity of the analysis, whereas the CL images only present a two-dimensional view of the zircon surface.

Mass discrimination effects were corrected using an exponential law. The mass bias factor for Hf was calculated by normalizing the measured $^{179}Hf/^{177}Hf$ to 0.7325 (Patchett et al., 1981). To obtain accurate $^{176}Hf/^{177}Hf$ for zircon, the contribution of isobaric interferences by ^{176}Lu and ^{176}Yb on the ^{176}Hf signal must be carefully corrected. The interferences were corrected by measuring ^{175}Lu and ^{173}Yb. The signal intensity of ^{176}Hf was calculated by

$$I_{^{176}\mathrm{Hf}} = I_{^{176}(\mathrm{Lu+Yb+Hf})} - \left[I_{^{175}\mathrm{Lu}} \times R^{\mathrm{true}}_{^{176}\mathrm{Lu}/^{175}\mathrm{Lu}} \times \left(\frac{m_{^{176}\mathrm{Lu}}}{m_{^{175}\mathrm{Lu}}} \right)^{\beta\mathrm{Lu}} + I_{^{173}\mathrm{Yb}} \times R^{\mathrm{true}}_{^{176}\mathrm{Yb}/^{173}\mathrm{Yb}} \times \left(\frac{m_{^{176}\mathrm{Yb}}}{m_{^{173}\mathrm{Yb}}} \right)^{\beta(\mathrm{Yb})} \right] \quad (1)$$

where I_i and m_i are signal intensity and mass of isotope i, R^{meas}, and R^{true} are true and measured isotope ratios, and β(Lu) and β(Yb) are mass bias factors for Lu and Yb, respectively. The true $^{176}Lu/^{175}Lu$ value of 0.026549 (Chu et al., 2002) and $^{176}Yb/^{173}Yb$ value of 0.78696 (Thirlwall and Anczkiewicz, 2004) were employed. The β(Yb) was calculated by normalizing the measured $^{173}Yb/^{171}Yb$ to 1.12346 (Thirlwall and Anczkiewicz, 2004), whereas the β(Lu) was assumed to be identical to the β(Hf). More detailed instrumental setting and analytical procedures are described in Iizuka and Hirata (2005).

We have accumulated Lu–Hf isotopic data for the zircon standard 91500, which is one of the most widely distributed and therefore extensively investigated standards for Lu–Hf isotopes by TIMS (Wiedenbeck et al., 1995) and solution MC-ICPMS (Amelin et al., 2000; Woodhead et al., 2004; Davis et al., 2005; Nebel-Jacobsen et al., 2005; Richards et al., 2005; Wu et al., 2006; Blichert-Toft, 2008, also see discussion by Griffin et al., 2006, 2007; Corfu, 2007). Our long term repeated analysis, using 63 μm pit size with 8 Hz repetition rate or 35 μm pit size with ~20 Hz repetition rates, yields an initial $^{176}Hf/^{177}Hf$ value of 0.282311 ± 50 (2 s.d.) (Table 2). The initial $^{176}Hf/^{177}Hf$ value is somewhat higher than a reference value of 0.282299 ± 6, which is calculated from the present-day $^{176}Hf/^{177}Hf$ value of 0.282305 ± 6 (Blichert-Toft, 2008: normalized to $^{176}Hf/^{177}Hf = 0.282160$ for JMC-Hf 475) and $^{176}Lu/^{177}Hf$ value of 0.00030 ± 3 obtained from the mean values of solution chemistry studies, even though the relative difference is smaller than the error. To allow accurate comparison with literature values, our Hf isotopic data were normalized to a value of 0.282299 for the 91500 standard, using the mean initial $^{176}Hf/^{177}Hf$ values obtained for this standard on any given day.

To evaluate the accuracy and precision of data obtained by the present technique, we have analyzed the zircon standards QGNG and TEMORA with the same analytical conditions as this study. Our determinations of the initial $^{176}Hf/^{177}Hf$ for QGNG (0.281588 ± 37, 2 s.d.) and for TEMORA (0.282678 ± 34, 2 s.d.) compare well with the solution-MC-ICPMS results for QGNG (0.281586 ± 4, calculated from $^{176}Lu/^{177}Hf = 0.000731$ and present-day

Table 2
Results from Lu–Hf isotopic analyses of the zircon sandards.

Zircon	Age (Ma)	$^{176}Lu/^{177}Hf$ (2 s.d.)	$^{176}Yb/^{177}Hf$ (2 s.d.)	$^{176}Hf/^{177}Hf$ (2 s.d.)	Initial $^{176}Hf/^{177}Hf$ (2 s.d.)
91500	1065.4				
Long term averages ($n = 156$)		0.00032 ± 14	0.00852 ± 385	0.282317 ± 50	0.282311 ± 50
		(0.00013–0.00061)	(0.00293–0.02045)		
This study ($n = 47$)		0.00034 ± 15	0.00971 ± 568	0.282322 ± 55	0.282315 ± 54
TEMORA ($n = 12$)	416.8	0.00108 ± 58	0.03337 ± 1736	0.282687 ± 35	0.282678 ± 34
		(0.00054–0.00146)	(0.01707–0.04265)		
QGNG ($n = 10$)	1851.6	0.00075 ± 42	0.02826 ± 1602	0.281649 ± 46	0.281622 ± 37
		(0.00040–0.00105)	(0.01401–0.03365)		

$^{176}Hf/^{177}Hf = 0.281612 \pm 4$ reported by Woodhead and Hergt, 2005) and TEMORA (0.282677 ± 8, calculated from $^{176}Lu/^{177}Hf = 0.00109$ and present-day $^{176}Hf/^{177}Hf = 0.282686 \pm 8$ reported by Woodhead and Hergt, 2005), respectively (Table 2). This indicates that the present analytical protocols are robust under *in situ* analysis of moderate to high heavy rare earth elements (REE)/Hf zircon.

We report analytical errors on the initial $^{176}Hf/^{177}Hf$, rather than the present-day $^{176}Hf/^{177}Hf$, for single spot measurements, because resolvable variations in the present-day $^{176}Hf/^{177}Hf$ due to radiogenic in-growth of ^{176}Hf may exist within Archean zircon grains having heterogeneous Lu/Hf. The analytical errors combine the internal run errors (2 s.e.) and the reproducibility of the standard analyses (2 s.d.), added in quadrature.

The calculation of the $^{176}Hf/^{177}Hf$ at a given time used the ^{176}Lu decay constant of 1.867×10^{-11} yr^{-1} (Söderlund et al., 2004). The present-day chondritic parameters reported by Bouvier et al. (2008) were used to calculate $\varepsilon Hf(t)$. To estimate the mean mantle-extraction age of the source materials of the zircon, we calculate depleted mantle two-stage model ages (T_{DM}) for all grains, under the assumption that the host magmas of the zircons were produced from crustal materials that were originally extracted from the depleted mantle. For the calculation, we used the $^{176}Lu/^{177}Hf$ of average Precambrian granitoid crust (0.0093; Vervoort and Patchett, 1996) for the reworked crustal materials. The depleted mantle evolution curve was defined by

$$\left[{}^{176}Hf/{}^{177}Hf\right]_t^{DM} = 0.2832 + 0.0393 \times (1 - e^{\lambda t}) \times (t \leqslant 3.76\ \text{Ga})$$
$$\left[{}^{176}Hf/{}^{177}Hf\right]_t^{DM} = \left[{}^{176}Hf/{}^{177}Hf\right]_t^{CHUR}\ (t > 3.76\ \text{Ga}) \quad (2)$$

where acronyms DM and CHUR represent depleted mantle and chondritic uniform reservoirs, respectively. The defined evolution curve is consistent with the Hf isotopic composition of juvenile rocks through time (Nowell et al., 1998; Blichert-Toft et al., 1999; Vervoort and Blichert-Toft, 1999; Davis et al., 2005). The assumption that the early mantle had chondritic Hf isotopic composition is also consistent with the lack of ancient (>3.76 Ga) zircons having positive $\varepsilon Hf(t)$ (Amelin et al., 1999, 2000; Blichert-Toft and Albarède, 2008; Harrison et al., 2008; Hiess et al., 2009; Iizuka et al., 2009). For grains having higher initial $^{176}Hf/^{177}Hf$ than the depleted mantle value, the U–Pb ages were interpreted as the mean mantle-extraction model ages.

3. RESULTS

3.1. U–Pb isotopic and trace element data

The U–Pb isotopic data for zircons are summarized in Electronic Annex Table EA-1. The data are also graphically presented on concordia diagrams for each river (Fig. 2). The zircon U–Pb age populations for each river are shown in histograms (Fig. 3a–d). Zircons having U–Pb ages older than 3.4 Ga were not observed in any sample studied. The Mississippi River zircons (MP1) define three major U–Pb age groups (Figs. 2a and 3a): (1) concordant and variably discordant zircons yielding $^{207}Pb/^{206}Pb$ ages of 2.8–2.6 Ga; (2) concordant and slightly discordant zircons defining ages between 1.8 and 0.9 Ga; (3) concordant zircons younger than 0.2 Ga (Iizuka et al., 2005). Most of zircons from the Congo (CNG2) and Yangtze (YZ1) Rivers yielded concordant or slightly discordant ages (Fig. 2b and c). The CNG2 data exhibit five peaks at 2.7–2.6, 2.1–1.8, 1.2–1.0, 0.8–0.5, and 0.3–0.2 Ga (Fig. 3b). The YZ1 data show small peaks at 2.7–2.4 and 2.0–1.8 Ga and prominent peaks at 0.9–0.7 and 0.3–0.1 Ga (Fig. 3c). The zircons from the Amazon River (AMZ8) can be characterized by two main groups of ages with concordant or variably discordant ages of 2.7–2.5 and 2.3–1.9 Ga (Figs. 2d and 3d). These U–Pb age distributions of the four rivers are, in general speaking, similar to those observed by Rino et al. (2004, 2008). In derail, however, this study resolved more prominent sharp peaks in the Phanerozoic era. This discrepancy is attributed to the difference in data handling of the young zircons: in this study we utilized $^{206}Pb/^{238}U$ ages for zircons younger than 1.0 Ga zircons, whereas Rino et al. (2004, 2008) used imprecise $^{207}Pb/^{206}Pb$ ages, thereby defining much broader peaks for the young zircon populations.

Some zircons older than 1.0 Ga are clearly discordant in terms of their U–Pb isotopes, suggesting that they have experienced Pb-loss events. Because inaccurate U–Pb ages would result in artificial secular trends of the geochemical and Hf isotopic compositions, we have not used the data obtained from >1.0 Ga with >25% discordance for the following discussion.

The trace element data for zircons are shown in Electronic Annex Table EA-2. Fig. 4 shows Hf, Yb, U, Ce/Ce*, Eu/Eu*, Yb/Sm and Th/U plotted against U–Pb age (Ce* and Eu* are theoretical Ce and Eu value predicted from a smooth chondrite-normalized REE pattern, respectively). Most zircons display REE patterns having positive Ce and negative Eu anomalies and a prominent heavy REEs enrichment relative to light and middle REEs, which

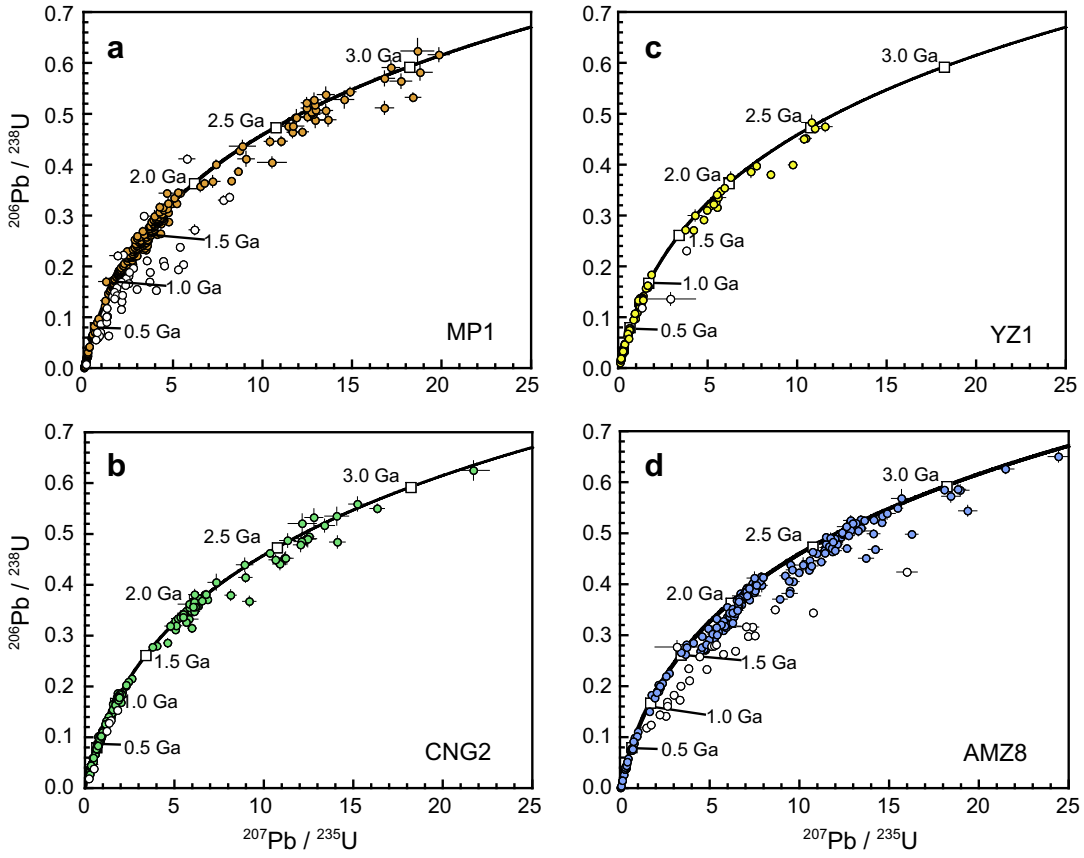

Fig. 2. U–Pb Concordia diagrams for detrital zircons from samples (a) MP1, (b) CNG2, (c) YZ1, and (d) AMZ8, respectively. Error bars represent errors quoted in Table EA-1. Open symbols indicate the data yielding >1.0 Ga $^{207}Pb/^{206}Pb$ ages with >25% discordance.

are commonly observed in terrestrial crustal zircons (e.g., Hoskin and Ireland, 2000). Furthermore, most zircons have Th/U of >0.1, a feature typical of magmatic zircons (Hoskin and Ireland, 2000; Rubatto, 2002).

3.2. Lu–Hf isotopic data

The Lu–Hf isotopic data obtained for the dated zircons are summarized in Electronic Annex Table EA-3. The zircon Lu–Hf isotopic data are also plotted as a function of their crystallization age (Figs. 5 and 6a). Fig. 5 illustrates that younger detrital zircons generally have higher initial $^{176}Hf/^{177}Hf$, and shows no clear horizontal trends which can be formed by various degree of ancient Pb loss from a single population of zircon (e.g., Amelin et al., 2000; Gerdes and Zeh, 2009; Iizuka et al., 2009). The Mississippi River zircons display four characteristics: (1) the zircons having Archean ages (>2.5 Ga) plot slightly above to clearly below the CHUR evolution curve with $\varepsilon Hf(t)$ values from +5 to −17; (2) the zircons with ages of around 2.5–1.8 Ga plot on to markedly below the CHUR curve; (3) most of the middle-late Proterozoic (1.8–0.9 Ga) zircons lie between the CHUR and DM evolution curves (positive $\varepsilon Hf(t)$); (4) the Phanerozoic zircons show a large spread in $\varepsilon Hf(t)$ values from +9 to −36 (Iizuka et al., 2005). The Congo River zircons can be characterized as follow: (1) the Archean zircons have $\varepsilon Hf(t)$ values from slightly positive to moderately negative values (+3 to −7); (2) the zircons with ages around 2.2–1.8 Ga mainly plot below the CHUR evolution curve and range in $\varepsilon Hf(t)$ values from +3 to −18; (3) the zircons crystallized after the late Proterozoic (<1.3 Ga) have clearly positive to negative $\varepsilon Hf(t)$ values (+9 to −30). The Yangtze River zircons have four characteristics: (1) all the Archean aged zircons except for one plot on to moderately above the CHUR evolution curve, with a range of $\varepsilon Hf(t)$ from +7 to −1; (2) the zircons with early Proterozoic ages (2.2–1.6 Ga) range in $\varepsilon Hf(t)$ from +2 to −14; (3) the zircons with ages around 1.1–0.6 Ga have a wide range of $\varepsilon Hf(t)$ values from +11 to −19; (4) most of the Phanerozoic zircons plot below the CHUR evolution curve with $\varepsilon Hf(t)$ values down to −34. The zircons from the Amazon River show three characteristics: (1) the $\varepsilon Hf(t)$ values for the Archean zircons range from +6 to -15 and indicate a peak between −5 and −10; (2) the zircons with ages around 2.3–1.9 Ga also mainly plot below the CHUR evolution curve, exhibiting a range of $\varepsilon Hf(t)$ from +3 to −21; (3) most of the zircons younger than 1.8 Ga yield $\varepsilon Hf(t)$ values from slightly positive to moderately negative.

The T_{DM} populations of the zircons are shown in histograms for each river (Fig. 3e–h). The T_{DM} for the Mississippi River zircons range from 3.6 to 0.2 Ga and indicate a low peak at 3.2–2.8 Ga and a broad peak between 2.1 and 0.9 Ga (Fig. 3e) (Iizuka et al., 2005). The T_{DM} for the Congo River zircons distribute between 3.4 and 0.7 Ga and show two broad peaks at 3.0–2.1 and 2.0–0.9 Ga (Fig. 3f). The Yangtze River zircons exhibit a range in T_{DM} from 3.1 to

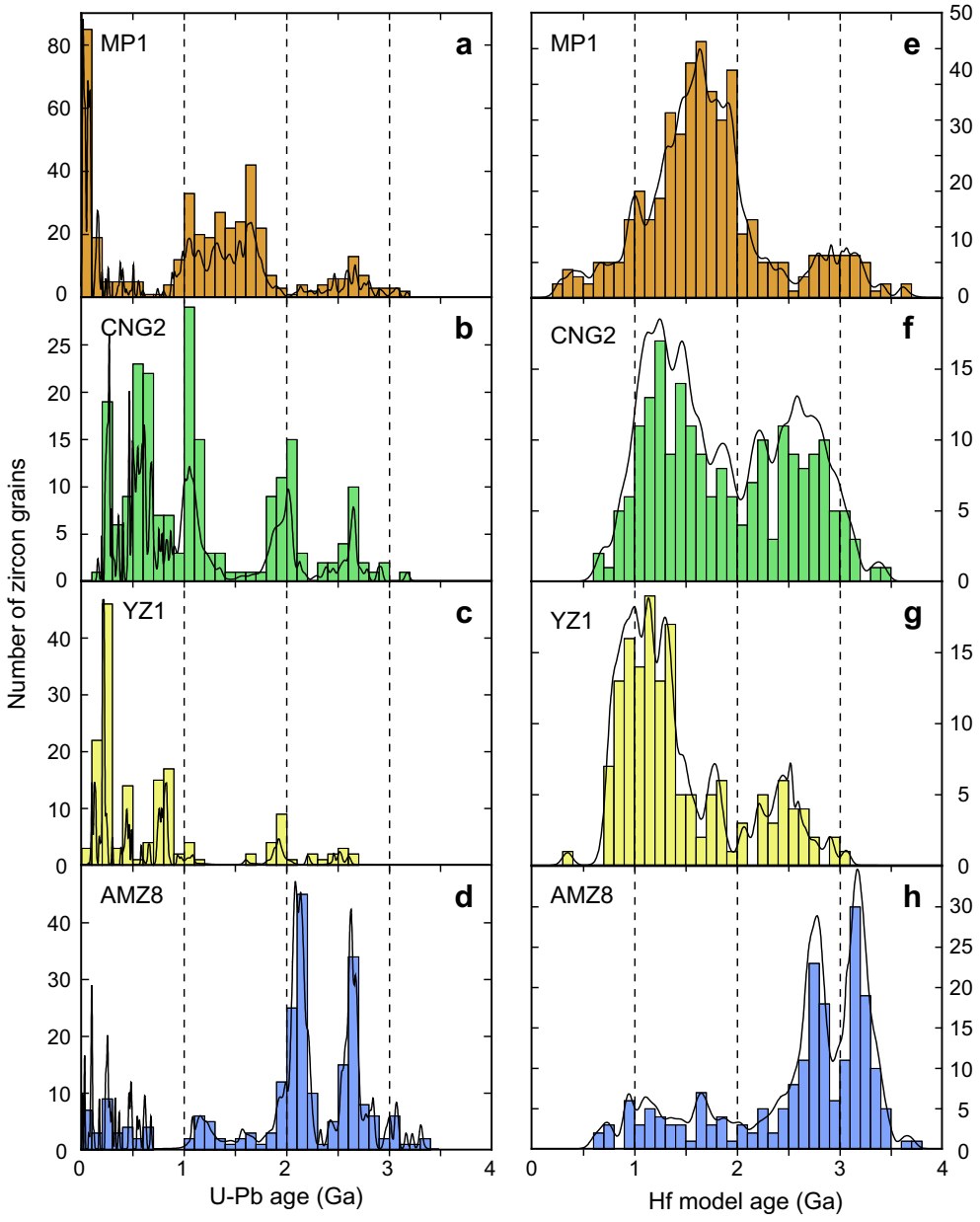

Fig. 3. (a–d) Histograms of U–Pb ages of detrital zircons from samples MP1, CNG2, YZ1, and AMZ8, respectively. (e–h) Histograms of Hf model ages (T_{DM}) of detrital zircons from the four samples. Hf model ages were calculated using a Lu/Hf of granitoid crust (Lu/Hf = 0.0093; Vervoort and Patchett, 1996). Solid lines show probability density plots.

0.4 Ga, with peaks at 2.7–2.4 and 1.4–0.7 Ga (Fig. 3g). The Amazon River zircons display a range in T_{DM} from 3.6 to 0.6 Ga and shows sharp peaks at 3.3–3.0 and 2.9–2.6 Ga (Fig. 3h). The zircon T_{DM} histograms for the four rivers (Fig. 3e–h) display no peaks in the Phanerozoic era.

4. DETRITAL ZIRCON U–PB ISOTOPE SYSTEMATICS

4.1. Provenance of detrital zircons

To evaluate the significance of U–Pb and Lu–Hf isotope systematics of detrital zircons in sand from large river systems, it is important to identify their mode of provenance. There are three main factors to be considered:

(1) Since zircon is ubiquitous as an accessory mineral in granitoid rocks that dominate the upper continental crust, they are most likely the original primary source of detrital zircons in river sands and sedimentary rocks.
(2) When considering the topography of the present-day continental crust, there is a tendency for young crust to be elevated in mountain belts, whilst older crust is generally flat and topographically sterile. This would tend to bias the erosion of young igneous rocks into

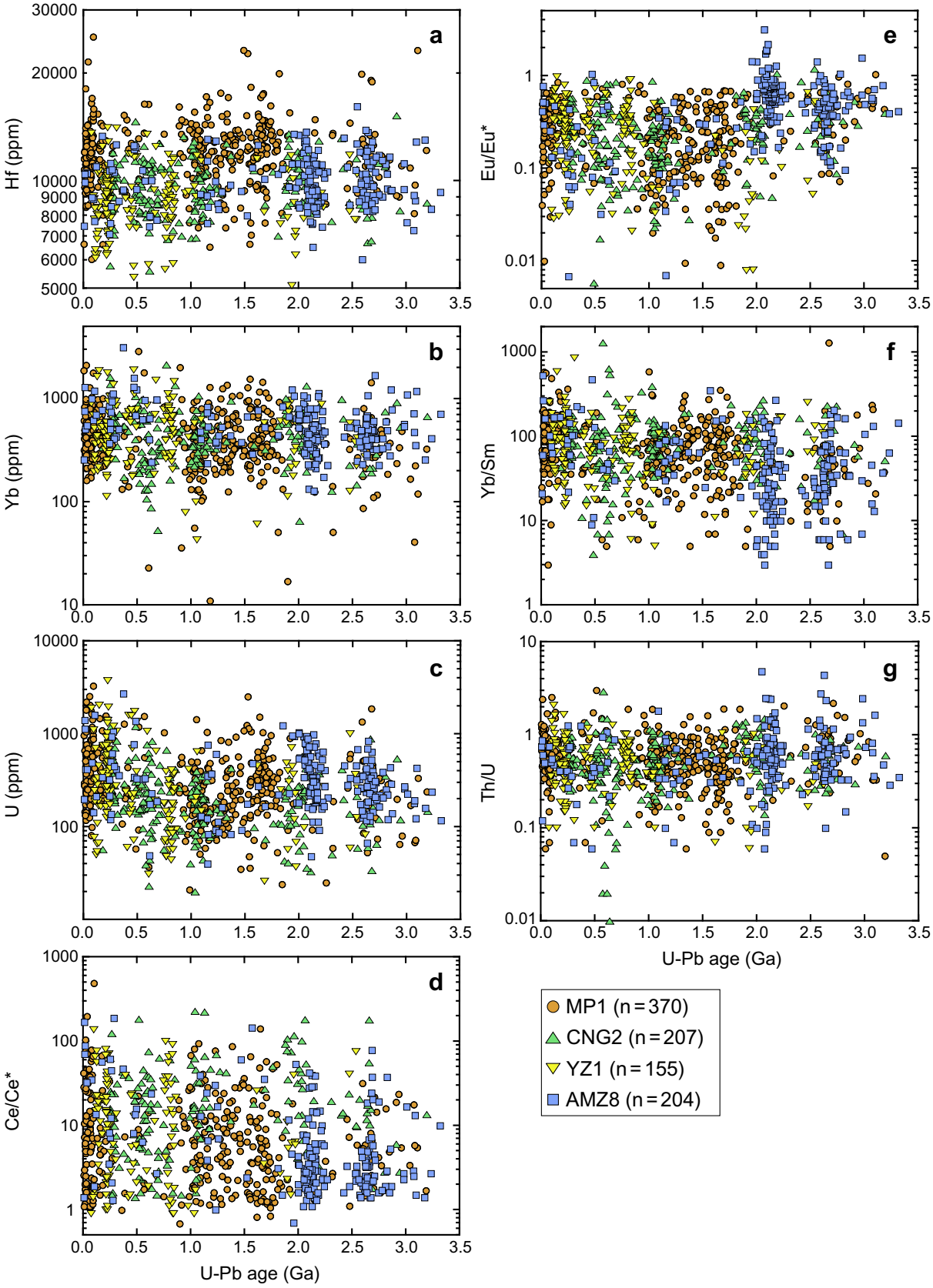

Fig. 4. Diagrams showing trace element compositions of detrital zircons studied here as a function of their crystallization age.

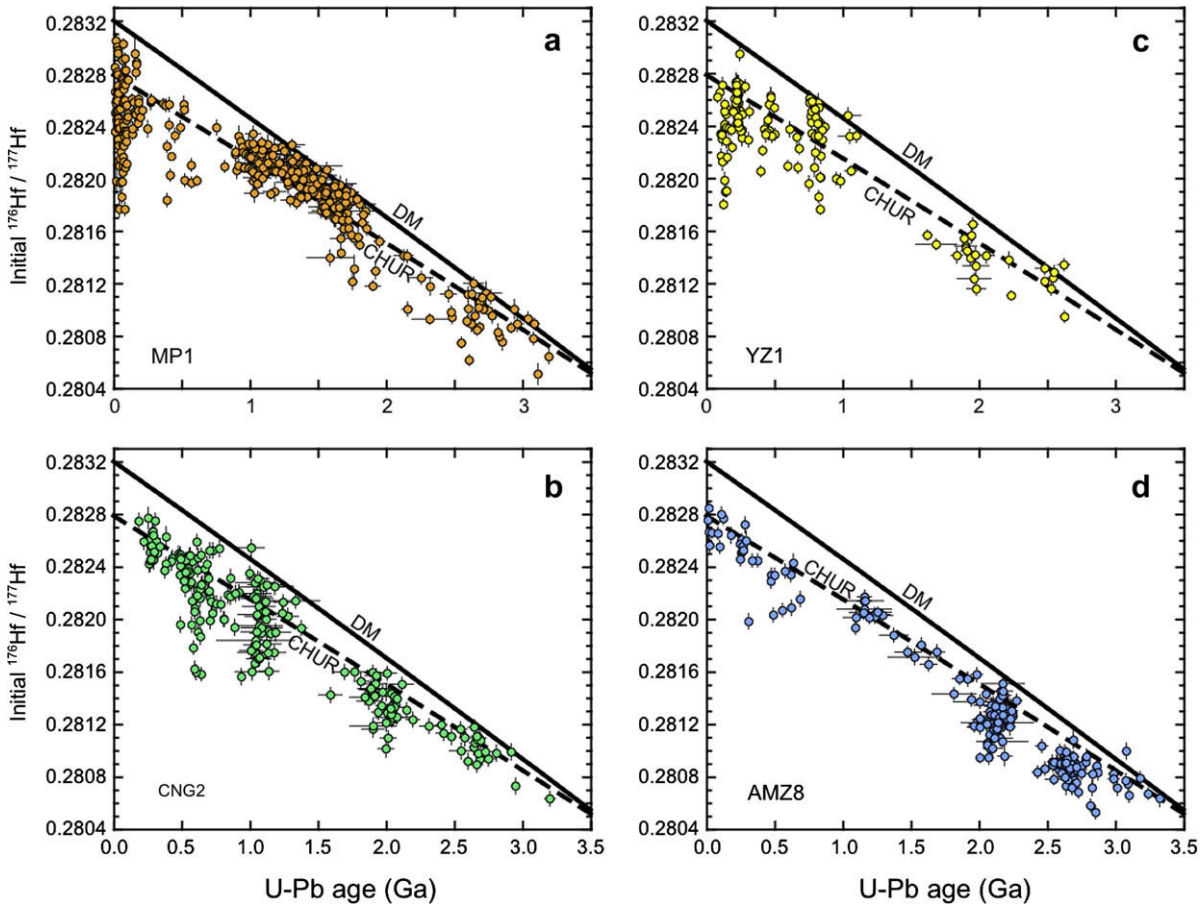

Fig. 5. Plots of initial $^{176}Hf/^{177}Hf$ versus U–Pb age for detrital zircons from samples (a) MP1, (b) CNG2, (c) YZ1, and (d) AMZ8, respectively. Chondritic uniform reservoir (CHUR) and depleted mantle (DM) evolution curves are also shown. Error bars represent errors quoted in Table EA-3.

sedimentary cycling over their older counterparts (Allègre and Rousseau, 1984; McLennan, 1988; Pinet and Souriau, 1988; Summerfield and Hulton, 1994).

(3) Sedimentary rocks are the most abundant rock type on the continental surface. They are disaggregated by wind and water more readily than igneous rocks, and therefore the rate of sedimentary recycling is much faster than the erosion of igneous basements, especially for old topographically sterile crust (Veizer and Jansen, 1979, 1985; Goldstein et al., 1984; Michard et al., 1985; McLennan, 1988; Veizer and Mackenzie, 2003).

Accordingly, it is logical to expect that zircons in sands from large river systems, as well as those in continental sedimentary rocks, were essentially derived from older sedimentary rocks (sedimentary recycling) and young contemporaneous granitoids (first-cycling). This inference is supported by the detrital zircon studies that have combined U–Pb isotopic dating with fission-track (FT) or U–Th–He isotopic dating.

The FT and U–Th–He isotope systems in zircon are effectively stable at <200 °C (e.g., Tagami et al., 1998; Reiners et al., 2004). These systems therefore can be used to date orogenic (exhumation) event that freed the zircon from its bedrock source for capture in the sampled sediments. By contrast, the U–Pb isotope system in zircon, having an effective closure temperature in excess of 900 °C (Lee et al., 1997; Cherniak and Watson, 2001), essentially records the time of its crystallization in the igneous rock. The combination of these low- and high-temperature zircon chronologies has revealed that zircons with old (>400 Ma) FT or U–Th–He ages are extremely rare in continental sediments such as those from the Mississippi, Gange and Indus Rivers (Carter and Moss, 1999; Carter and Bristow, 2000; Rahl et al., 2003; Campbell et al., 2005; Reiners et al., 2005). This finding is consistent with the view that first-cycle zircons derived from old igneous basements are minor. Furthermore, by coupling the detrital zircon He–Pb isotopic data with reported geochronological data for the source regions, it is indicated that at least 70% of the Navajo sandstone and Ganges River and 60% of the Indus River zircons have been recycled from earlier sediments, and that the proportions of first-cycle zircons derived from old (>300 Ma) igneous basements are <7% and 0–27% for the Ganges and Indus River sands, respectively (Rahl et al., 2003; Campbell et al., 2005).

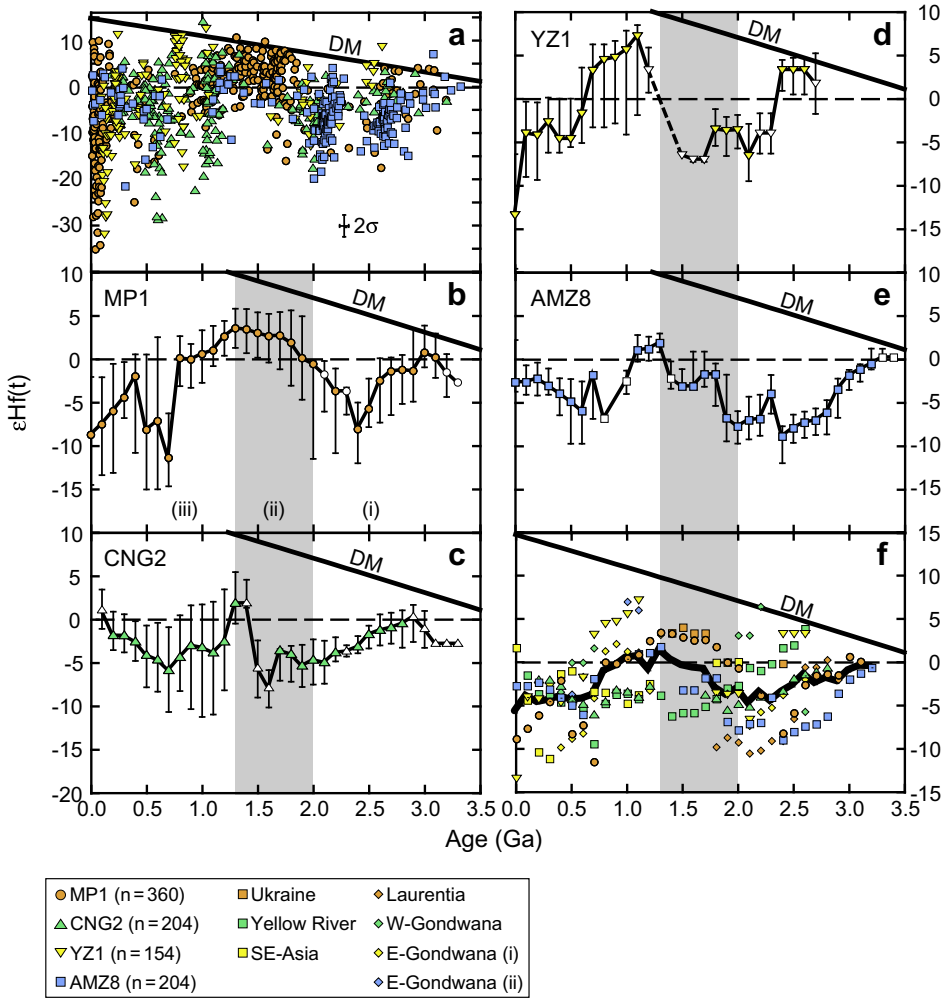

Fig. 6. Secular variations in $\varepsilon Hf(t)$ for detrital zircons. (a) Plot of $\varepsilon Hf(t)$ versus U–Pb age for zircons from samples of this study. The average 2σ uncertainty is also represented. Depleted mantle (DM) evolution curve is also shown. (b–e) Running median trends for zircons from each sample of this study based on a 300 Ma window and 100 Ma forward step. Medians calculated from <5 data sets are represented with open symbols. Vertical bars depict interquartile ranges (from first quartile to third quartile). The deviation of $\varepsilon Hf(t)$ between detrital zircons and the depleted mantle ($\Delta\varepsilon Hf_{DM}(t)$) increased from the Mesoarchaean to early Paleoproterozoic (i), and decreased during Paleo- and Mesoproterozoic time (ii). and again increased toward the present (iii). Gray bands show the period (ii) that $\Delta\varepsilon Hf_{DM}(t)$ decreased. (f) Compilation of the running medians for zircons from the samples of this study and from river sands of other large rivers in Southeast-Asia (Bodet and Schärer, 2000), the Ukraine (Condie et al., 2005), and China (Yang et al., 2009) and sedimentary rocks deposited on the passive margins of the Laurentian (Condie et al., 2005), West-Gondwana (Gerdes and Zeh, 2006), and East-Gondwana (i, Kemp et al., 2006; ii, Veevers et al., 2006) continents. Medians based on <5 data sets have been omitted. The solid line shows the mean of the running medians (Table 4).

4.2. U–Pb age distribution

The oldest of our zircons in all river sands except for YZ1 have U–Pb ages of circa 3.3 Ga (Fig. 3a–d). This indicates the ubiquitous granitoid crust formation by around 3.3 Ga, and also implies that sedimentary recycling has been operative since that time, thereby preserving circa 3.3 Ga zircons in modern sediments widely. It should be noted that the paucity of >3.3 Ga detrital zircons has been commonly recognized for other large rivers (Ledent et al., 1964; Goldstein et al., 1997; Bodet and Schärer, 2000; Rino et al., 2004, 2008; Amidon et al., 2005; Condie et al., 2005; Campbell and Allen, 2008; Yang et al., 2009).

Each river sand sample shows several prominent peaks in the zircon U–Pb age histogram. Notably, a peak at 2.7–2.5 Ga was observed in all the four river zircons. This, as well as the widespread occurrence of granitoids with ages of circa 2.7 Ga at present (Gastil, 1960), suggests global episodic granitoid formation during this period. Another commonly-observed feature in all the U–Pb age histograms is a lack of ages at 2.4–2.2 Ga, indicating a globally quiescent period of granitoid crust formation during this period. In addition, the few 2.4–2.2 Ga zircons all have negative $\varepsilon Hf(t)$ values (Fig. 6a), suggesting little crust generation in the time interval. Such a phenomenon was recently highlighted by Condie et al. (2009). On the other hand, there is no

synchronization of post-Archean peaks amongst the four samples. This suggests that episodic granitoid formation in the source regions of the four river sands are not coincident in post-Archean era, in contrast to the episodic global granitoid formation at 2.7–2.5 Ga.

Fig. 7a shows the the probability density plot for the U–Pb ages of detrital zircons. The relative probability was based on the age proportions, rather than the number of grains, of detrital zircons from the four rivers thus avoiding undue weighting of the results based on the relatively large number of analyses (i.e., the relative probability of zircons having U–Pb ages between t and t–100 Ma is an average of percentages of the zircons for each river sand sample). We can recognize peaks at 2.7–2.5, 2.2–1.9, 1.7–1.6, 1.2–1.0, 0.9–0.4, and <0.3 Ga. These well correlate with the timing of aggregation of the Sclavia/Superia, Columbia, Rodinia, Gondwana, and Pangea supercontinents, respectively (Dalziel et al., 2000; Bleeker, 2003; Veevers, 2004; Zhao et al., 2004; Johnson et al., 2005; Cawood and Buchan, 2007; De Waele et al., 2008; Rogers and Santosh, 2009) (Fig. 7a). The correspondence can be interpreted as reflecting that the formations of supercontinents are coupled with episodic major igneous activities resulting from subducted slab avalanches and mantle instabilities (Condie, 1998; Rino et al., 2004, 2008) and/or that super-mountain building due to continental collisions enhanced first-cycling of young igneous basements to the sedimentary system (Campbell and Allen, 2008).

5. DETRITAL ZIRCON HF ISOTOPE SYSTEMATICS

5.1. Comparison with Nd isotopic data of river sediments

The Hf and Nd isotope systematics for the most crust and mantle form a strong correlation, indicating the covariance between Lu/Hf and Sm/Nd fractionations by most magmatic processes in the crust and mantle (Johnson and Beard, 1993; Vervoort and Blichert-Toft, 1999; Vervoort et al., 1999). To compare the present Hf isotopic data of detrital zircons with previously reported Nd isotopic data of sediments from the Mississippi, Yangtze, Congo, and Amazon Rivers, the averaged zircon T_{DM} values and Nd depleted mantle model ages of the sediments (Goldstein et al., 1984) are summarized in Table 3. The Nd model ages were calculated using the present $^{143}Nd/^{144}Nd$ and $^{147}Sm/^{144}Nd$ of the river sediments (Goldstein et al., 1984) with the Nd isotopic evolution line for the depleted mantle proposed by McLennan and Hemming (1992), which assumes that the mantle evolved progressively from $\varepsilon Nd(3.8\text{ Ga}) = 0$ to $\varepsilon Nd(\text{present}) = +10$.

For the Mississippi, Congo and Yangtze Rivers, the Nd model ages correspond to the averaged values of T_{DM} in the

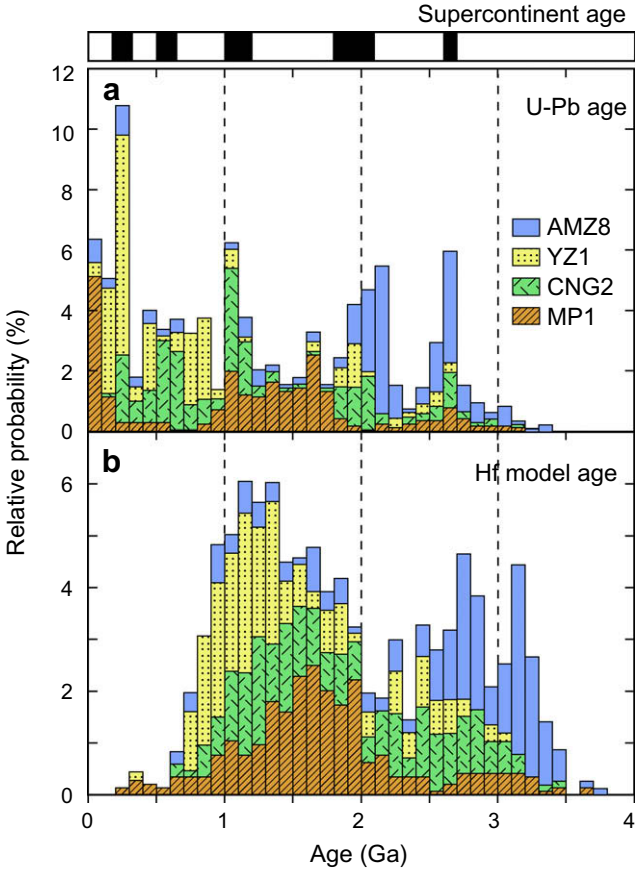

Fig. 7. Compiled (a) U–Pb and (b) Hf model (T_{DM}) age populations of detrital zircons from the four rivers. They were obtained by accumulating the age proportions rather than the number of grains of detrital zircons from the four rivers, to avoid undue weighting of the results based on the relatively large number of analyses. Periods of supercontinent assembly are shown in the top column.

Table 3
Comparison of average zircon Hf model ages and Nd model ages of sediments for the Mississippi, Yangtze, Congo, and Amazon Rivers.

River	Detrital zircon				Sediments*
	U–Pb age	1 s.d.	T_{DM}	1 s.d.	Nd model age
Mississippi	1.10	0.83	1.72	0.64	1.64
Congo	1.19	0.77	1.89	0.69	1.91
Yangtze	0.69	0.68	1.44	0.59	1.57, 1.62
Amazon	1.96	0.84	2.57	0.76	1.48

All ages are represented in Ga.
* Nd isotopic data are from Goldstein et al. (1984), which were recalculated with the depleted mantle evolution curve of McLennan and Hemming (1992).

range of 0.2 Ga. This clearly supports the point that the Hf and Nd isotope systematics are generally well coupled during most magmatic as well as sedimentary processes. By contrast, the Nd model age of the Amazon River sediments are 1.1 Ga younger than the average T_{DM} of the detrital zircons. There are two possible causes for this discrepancy. The first is that because zircon is highly resistant to chemical weathering relative to other minerals (Patchett et al., 1984; Velbel, 1999; Balan et al., 2001), Sm and Nd could be preferentially moved into, or out of, the sedimentary system during sedimentary cycle. We see no reason, however, that the decoupling owing to the high resistance of zircon could be significant only for the Amazon River. The second, and more plausible explanation, is that the Amazon River sediments certainly originated from igneous rocks that contain few zircons and have young depleted mantle model ages. In fact, the northern volcanic zone of the Andes, which represents an important contribution of sediment to the Amazon River (e.g., Dosseto et al., 2006), is mainly comprised of late Cenozoic undifferentiated rocks (basalt–basaltic andesite) with relatively juvenile isotopic signatures (Harmon et al., 1984; Thorpe et al., 1984).

5.2. Hf model age distribution

A plot of $\varepsilon Hf(t)$ against crystallization age (Fig. 6a) shows that most zircons have markedly lower $\varepsilon Hf(t)$ than

Table 4
Mean of the running median of zircon $\varepsilon Hf(t)$ for the river sands and sedimentary rocks.

Age (±0.15 Ga)	Mean $\varepsilon Hf(t)$[a]	1 s.d.	Model age[b] (Ga)	Data source[c]
0.0	−5.79	6.65	1.02	1, 3–5
0.1	−4.01	2.30	1.01	1, 3–5
0.2	−4.74	3.11	1.13	1–5
0.3	−4.49	3.34	1.20	1–5
0.4	−4.08	2.44	1.261	1–5, 7, 9–11
0.5	−4.43	2.87	1.35	1–5, 7, 9–11
0.6	−4.35	2.92	1.43	1–4, 7, 9–11
0.7	−3.90	5.03	1.48	1–5, 7, 9, 11
0.8	−1.13	3.70	1.43	1–3, 5, 7, 11
0.9	−0.57	3.46	1.48	1–3, 5, 10
1.0	0.41	4.60	1.51	1–3, 5, 7, 10, 11
1.1	0.56	4.41	1.59	1–5, 7, 10, 11
1.2	−0.93	2.58	1.74	1, 2, 4, 5, 11
1.3	1.31	2.95	1.71	1, 2, 4, 7, 11
1.4	0.20	5.52	1.84	1, 6, 7
1.5	−0.48	4.76	1.96	1, 4, 6, 7
1.6	−0.75	4.48	2.05	1, 4, 6, 7
1.7	−0.90	3.77	2.14	1, 2, 4, 6, 7
1.8	−3.07	3.71	2.32	1–5, 7, 8
1.9	−3.88	3.07	2.44	1–5, 7–9
2.0	−3.18	4.10	2.49	1–5, 7–9
2.1	−4.84	4.60	2.65	2–4, 7–9, 11
2.2	−3.55	5.27	2.67	1, 2, 4, 7–9, 11
2.3	−4.60	3.67	2.79	4, 7, 8, 11
2.4	−3.53	4.88	2.82	1–4, 6, 7, 8, 11
2.5	−2.79	4.71	2.87	1–4, 7, 8
2.6	−1.52	3.89	2.89	1–4, 7–9, 11
2.7	−2.53	3.06	2.02	1, 2, 4, 8
2.8	−1.94	2.91	3.07	1, 2, 4, 8
2.9	−2.32	1.10	3.17	1, 4, 8
3.0	−1.07	1.53	3.19	1, 4, 8
3.1	−0.55	0.95	3.25	1, 4
3.2	−0.59		3.33	4

[a] The medians based on <5 data set have been left out.
[b] Calculated using the ratio of average Precambrian granitoid crust ($^{176}Lu/^{177}Hf = 0.0093$: Vervoort and Patchett, 1996).
[c] (1) MP1; (2) CNG2; (3) YZ1; (4) AMZ8; (5) SE-Asia; (6) Ukrain; (7) Yellow River; (8) Laurentia; (9) W-Gondwana; (10 and 11) E-Gondwana (i) and (ii).

that of the depleted mantle at the time of crystallization. In detail, the proportions of all zircons having crustal residence time (the deviation of T_{DM} from the U–Pb age) of >300 Ma from the Mississippi, Yangtze, Congo, and Amazon River sands are 69%, 85%, 86%, and 90%, respectively. These data reinforce the view that granitoid magmatism has had a fundamental role in the differentiation of the continental crust. The relatively short average crustal residence time for the Mississippi River is due to the high proportion of 1.8–1.3 Ga zircons that generally have high $\varepsilon Hf(t)$. The figure also illustrates the significance of crustal reworking in granitoid formation even before 2.8 Ga, indicating that crust, which was stable for long enough to result in a significant change in Hf isotopes, was present by Mesoarchaean time.

Zircon Hf model age (T_{DM}) can provide chronological constraints on the generation of juvenile continental crust that was reworked into the zircon parental magma. However, the T_{DM} potentially represents the accurate timing of the crust generation only if the parental magma lacked a mixed component (Arndt and Goldstein, 1987); if not, then the T_{DM} provides the hybrid age of multi components. Indeed, recent studies (e.g., Grove et al., 1997; Annen et al., 2006; Kemp et al., 2007; Jagoutz et al., 2009) have demonstrated that many granitoid magmas contain not only a crustal source component but also a juvenile mantle source component. In addition, parental magmas of some granitoids, such as S-type granites, certainly involve multi-crustal components having various Lu/Hf ratios (e.g., Chappell, 1984). Since the T_{DM} is calculated under the assumption that the reworked crust is granitoid in Lu/Hf composition ($^{176}Lu/^{177}Hf = 0.0093$; Vervoort and Patchett, 1996), this can only be regarded as a minimum age for the reworked crust (Nebel et al., 2007). Note that even a combination of zircon Hf and O isotopes (Kemp et al., 2006; Pietranik et al., 2008; Hiess et al., 2009; Wang et al., 2009) cannot circumvent the former problem, though it can diagnose reworking of a sedimentary source component.

We draw attention to three features in the T_{DM} distribution (Fig. 3e–h). The first is that the oldest zircon T_{DM} for the Mississippi, Congo and Amazon River sands, are circa 3.7 Ga. This suggests that crust generation generally took place by around 3.7 Ga, and that the crusts were subsequently reworked into <3.3 Ga granitoid crusts. The second feature is that the model age histograms for the four river zircons show no peaks in the Phanerozoic era. This is in contrast to the prominent peaks in the same time interval in the U–Pb age histograms (Fig. 3a–d), indicating that Precambrian continental crusts were dominant sources of Phanerozoic granitoid magmas. The third feature is that all of the four river samples show peaks between 3.4 and 2.4 Ga and between 2.0 and 0.8 Ga, indicating that sources of large volume of granitoid continental crust are, on an average, extracted from the mantle during these periods. The broadness of the peaks, relative to those in the U–Pb age distributions, can be interpreted as reflecting either that generation of the continental crust is less episodic as compared to granitoid crust formation, or that the granitoid magmas have mixed age source rocks.

The accumulated T_{DM} population of detrital zircons from the four rivers (Fig. 7b) shows relatively sharp peaks at 3.3–3.0 and 2.9–2.4 Ga, and a broad peak between 2.0 and 0.9 Ga. These are broadly coincident with the observed peaks in the Nd model age population of sedimentary rocks (around 3.6, 2.7, 1.9, and 1.2 Ga; McCulloch and Bennett, 1994), and also with those in the Hf model age population of detrital zircons having mantle-like O isotope signatures (at 3.4–3.0 and 2.2–1.7 Ga; Kemp et al., 2006; Wang et al., 2009).

5.3. Secular variation of Hf isotopes in granitoid crust

Detrital zircons, even those having similar U–Pb ages, show a wide range in $\varepsilon Hf(t)$ (Fig. 6a), indicating that granitoid crust is highly heterogeneous in terms of radiogenic isotopes. To examine possible general secular change of radiogenic isotopes in zircons from large rivers, we have plotted running medians of $\varepsilon Hf(t)$, based on a 300 Ma window and 100 Ma forward step, for zircons from each sample of this study (Fig. 6b–e). Common characteristics have been identified: (i) the median $\varepsilon Hf(t)$ value deviates from the depleted mantle evolution curve from the Mesoarchaean to early Paleoproterozoic, (ii) the deviation ($\Delta\varepsilon Hf_{DM}(t)$) decreased between circa 2.0 and 1.3 Ga (gray bars on Fig. 6), and (iii) increased afterwards. Note that a choice of a 200 or 600 Ma window for the calculation would produce similar trends. To evaluate the further generality of the trends, we also calculated and plotted the $\varepsilon Hf(t)$ medians of zircons from other large river sands (Yellow River, Yang et al., 2009; Southeast-Asia, Bodet and Schärer, 2000; Ukaraine, Condie et al., 2005) and sedimentary rocks deposited on the passive margins of the continents, namely former river sands in large river systems (Laurentia, Condie et al., 2005; East-Gondwana, Kemp et al., 2006 and Veevers et al., 2006; West-Gondwana, Gerdes and Zeh, 2006) (Fig. 6f). The results indicate the similarity of the trends.

It might be possible that the noted trends are attributed to other mechanisms other than those associated with granitoid crust formation, such as the abundance of zircons derived from mafic rocks or sedimentary cycling processes. Zircons derived from mafic rocks tend to have relatively higher $\varepsilon Hf(t)$ and low Hf contents (Belousova et al., 2002). Preferential input of mafic-derived zircon in the 2.0–1.3 Ga period could account for the trends, but no systematic secular variations were observed in the Hf abundance in the zircons (Fig. 8a), suggesting this mechanism unlikely. If sedimentary processes were responsible, then it would require a global preferential cycling of zircons that have a certain $\varepsilon Hf(t)$ and a particular crystallization age. Such preferential sedimentary cycling could occur during collisional orogenesis, because continental collision would generate leucogranites having low $\varepsilon Hf(t)$ via intra-crustal melting (Deniel et al., 1987; France-Lanord and Le Fort, 1988; Inger and Harris, 1993) and subsequently uplift them to be preferentially eroded, whereas such granitoids are volumetrically minor. However, we see no correlation between the secular trends and the timing of aggregation of supercontinents (Figs. 6b–f and 7), suggesting that the preferen-

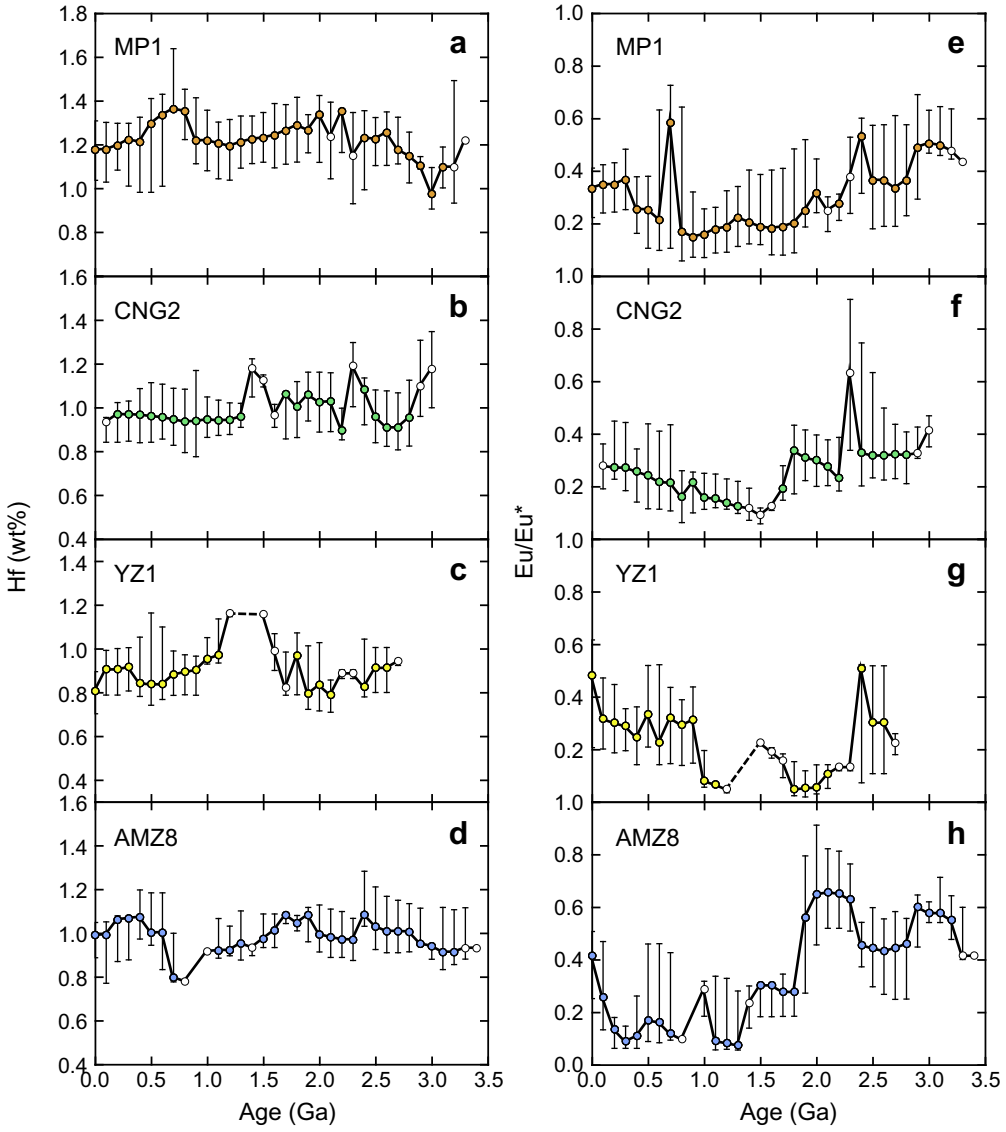

Fig. 8. Running medians (circles) and interquartile ranges (vertical bars) of (a) Hf contents and (b) Eu/Eu^* for detrital zircons from the four samples, based on a 300 Ma window and 100 Ma forward step. Medians based on <5 data sets are shown by open circles.

tial sedimentary process is not a dominant control. We therefore conclude that the trends reflect secular variations of Hf isotopes in granitoid crust.

5.4. Generation and differentiation of the continental crust

The geological significance of the observed $\varepsilon Hf(t)$ trends can be investigated by modelling the Hf isotopic evolution of granitoid crust in terms of the efficiency of crustal reworking. In the context of a granitoid genesis model in which a parental magma involves a juvenile magma component derived from the depleted mantle and a reworked crustal component (e.g., Grove et al., 1997; Annen et al., 2006; Kemp et al., 2007; Jagoutz et al., 2009), the $\varepsilon Hf(t)$ of the granitoid can be adequately estimated by adjusting the mass fraction of Hf from the reworked crustal component involved in the mixing. This is termed the reworking index. We have considered that crust formation events take place with a regular time interval of 100 Ma. The initial Hf isotope ratio of the granitoid crust formed during the nth event at time t_n is given by:

$$[^{176}Hf/^{177}Hf]^{GC}_{t_n} = \alpha_n[^{176}Hf/^{177}Hf]^{RC}_{t_n} + (1-\alpha_n) \times [^{176}Hf/^{177}Hf]^{DM}_{t_n} \quad (3)$$

where acronyms GC, RC, and DM represents the granitoid crust, reworked crustal component and depleted mantle, respectively, and α is the reworking index. Hence α reflects relative significance of the juvenile magma addition (crustal generation) and reworking of pre-existing crust (crustal differentiation) in granitoid crust formation. Because $[^{176}Hf/^{177}Hf]^{GC}_{t_n}$ is measured (Fig. 6b–f) and $[^{176}Hf/^{177}Hf]^{DM}_{t_n}$ is defined in Eq. (2), we can deduce α_n by assuming $[^{176}Hf/^{177}Hf]^{RC}_{t_n}$.

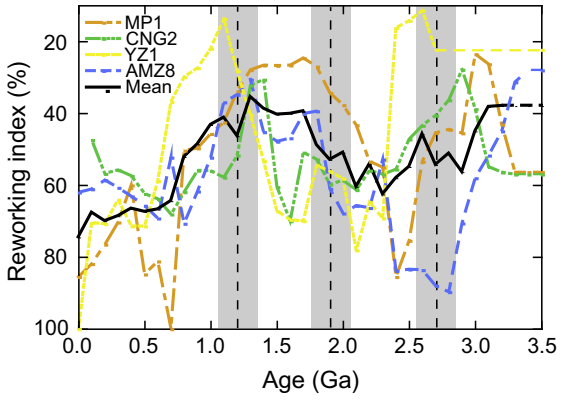

Fig. 9. Reworking index as a function of time, as modelled to reproduce the $\varepsilon Hf(t)$ trends in granitoid crusts (as in Fig. 6b–f). The model assumes that granitoid genesis results from a mixture between juvenile magmas and crustal melts derived from pre-existing crusts comprising granitoid and mafic rocks with crystallization ages from ~2000 to 100 Ma. The mass ratio of the mafic and granitoids is assumed to be 1 (see text for details). The time window (±150 Ma) used for the calculation of $\varepsilon Hf(t)$ medians is illustrated by the shaded zones surrounding the reference lines at 2.7, 1.9, and 1.2 Ga.

Since both mafic and granitoid (sedimentary) rocks are likely to be involved in the formation of granitoid crust (e.g., Chappell, 1984; Kemp et al., 2007), we have considered that the reworked crustal component is derived from pre-existing crusts comprising granitoid and mafic rocks with a certain mass ratio of the two rocks ($m_{mafic}/m_{granitoid}$). We then assume that the mafic rock has the Hf isotopic composition of the contemporaneous depleted mantle at the time of formation and has a $^{176}Lu/^{177}Hf$ of mafic lower crust (0.018; Rudnick and Fountain, 1995). For the granitoid, we have used the observed $\varepsilon Hf(t)$ for its initial Hf isotope ratio (Fig. 6b–f) and the $^{176}Lu/^{177}Hf$ of average Precambrian granitoid crust (0.0093; Vervoort and Patchett, 1996). For old granitoids in Fig. 6b–f where the $\varepsilon Hf(t)$ is not available, their initial Hf isotope ratios were taken to give $\Delta\varepsilon Hf_{DM}(t)$ equal to that of the oldest available granitoids in each sample (i.e., $\Delta\varepsilon Hf_{DM}(t)$ are 4.6 for >3.3 Ga MP1 granitoids, 4.7 for >3.3 Ga CNG2 granitoids, 2.5 for >2.7 Ga YZ1 granitoids, 1.3 for >3.4 Ga AMZ8 granitoids, and 1.9 for >3.2 Ga Mean granitoids, respectively). The Hf isotopic composition of the reworked crustal component is expressed as the following equations:

with

$$x = \frac{m_{granitoid} C^{Hf}_{granitoid}}{m_{granitoid} C^{Hf}_{granitoid} + m_{mafic} C^{Hf}_{mafic}} = \frac{1}{1 + (m_{mafic}/m_{granitoid})\left(C^{Hf}_{mafic}/C^{Hf}_{granitoid}\right)}$$

and

$$\sum_{0}^{n-1} a_i = 1 \quad (a_i \geqslant 0) \tag{4}$$

where a_i is the contribution of the pre-existing crust formed in the ith event to the reworked crustal component, and $C^{Hf}_{granitoid}$ and C^{Hf}_{mafic} are the concentrations of Hf in the granitoid and mafic rocks, respectively. The Hf contents of average Precambrian granitoid crust (9.0 ppm; Vervoort and Patchett, 1996) and of mafic lower crust (1.9 ppm; Rudnick and Fountain, 1995) were used for $C^{Hf}_{granitoid}$ and C^{Hf}_{mafic}, respectively. As we have no evidence for reworking of crust older than 3.7 Ga (Fig. 7b), our calculations start from 3700 Ma (i.e., $t_0 = 3700$ Ma). The parameters of a_i and $m_{mafic}/m_{granitoid}$ can be chosen in different ways. We tentatively accepted that pre-existing crusts available for reworking at any time are restricted to the ~20 last formed (~2000–100 Ma) crusts with a $m_{mafic}/m_{granitoid}$ of 1. Because the cumulative age distribution of geologic entities such as continental basement and sediments follows a power law function (Veizer and Jansen, 1985), the contribution of each crust has been taken to decrease with age:

$$\sum_{n-20}^{n-1} a_i = 1 \text{ and } \sum_{n-20}^{n-k} a_i = \left(\frac{21-k}{20}\right)^{3/2} \quad (n \geqslant 20)$$

$$\sum_{0}^{n-1} a_i = 1 \text{ and } \sum_{0}^{n-k} a_i = \left(\frac{n-k+1}{n}\right)^{3/2} \quad (n < 20) \tag{5}$$

We can then calculate $[^{176}Hf/^{177}Hf]^{RC}_{t_n}$ and obtain α_n. Beginning with the oldest ages, we estimated the successive α_n step by step and deduced the secular change in α. Fig. 9 shows the temporal change in the reworking index to reproduce the observed $\varepsilon Hf(t)$ curves in granitoid crusts (Figs. 6b–f). Note that the choice of an age range of 1000–100 or 3000–100 Ma and of a $m_{mafic}/m_{granitoid}$ value of 4 or 1/4 for reworked crust would not alter the arguments below (Fig. 10). The results indicate that increased reworking index is defined at >2.5 and 2.1–1.0 Ga for the Mississippi River zircons, >2.5 and 1.5–1.2 Ga for the Congo River zircons, >2.3 and 1.4–0.6 Ga for the Yangtze River zircons, >3.0 and 1.9–1.0 Ga for the Amazon River zircons, and >3.0 and 1.8–0.8 Ga for the mean of all detrital

$$[^{176}Hf/^{177}Hf]^{RC}_{t_n} = x\left[\sum_{0}^{n-1} a_i\left([^{176}Hf/^{177}Hf]^{GC}_{t_i} + [^{176}Lu/^{177}Hf]^{garnitoid}\left(e^{\lambda(t_i-t_n)}\right) - 1\right)\right]$$

$$+ (1-x)\left[\sum_{0}^{n-1} a_i\left([^{176}Hf/^{177}Hf]^{DM}_{t_i} + [^{176}Lu/^{177}Hf]^{mafic}\left(e^{\lambda(t_i-t_n)}\right) - 1\right)\right]$$

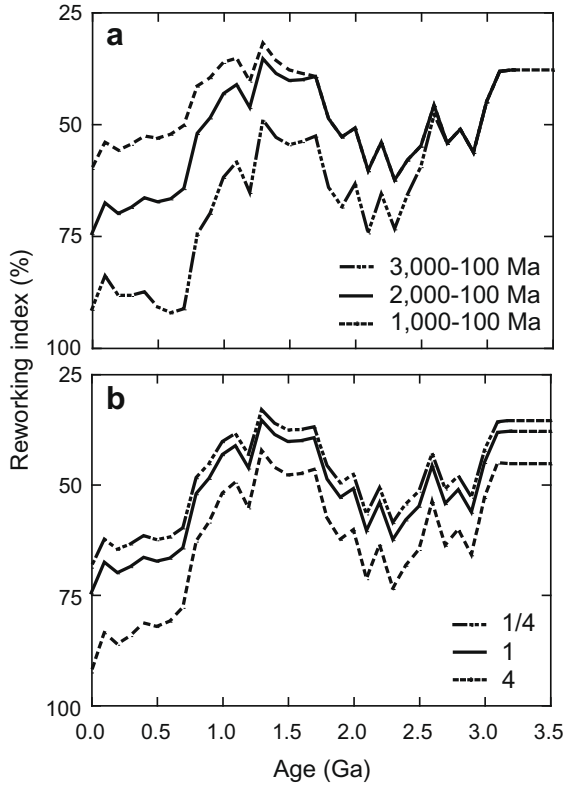

Fig. 10. Secular changes in reworking index to reproduce the εHf(t) trend in granitoid crust as in Fig. 6f and Table 4, based on the assumption that granitoid crust formation results from a mixture between a juvenile magma component and a reworked crustal component. (a) Pre-existing crusts available for reworking have the $m_{mafic}/m_{granitoid}$ value of 1, and an age range of ~1000–100, ~2000–100, or ~3000–100 Ma. (b) Pre-existing crusts available for reworking are restricted to ~2000–100 Ma crusts, which have a $m_{mafic}/m_{granitoid}$ value of 1/4, 1, or 4.

zircons from large rivers and continental sedimentary rocks (solid line in Fig. 6f and Table 4).

There are at least two plausible mechanisms capable of significantly changing the reworking index in granitoid crust formation with geological time. The first is the variation in rate of continental crust generation. Thermal simulations for granitoid genesis (Annen et al., 2006) show that a high basalt emplacement rate results in high production rates of both crustal melts and residual melts from basalt crystallization, but an increase of the crustal melting is restricted relative to the residual melting because heat diffusion in the crust limits the thickness of the crustal melted zone. This suggests that a reworking index would be relatively low in a period of rapid continental crust generation. The temporal variations of the reworking index therefore can be interpreted as indicating that the rate of crust generation increased around (or before) 3.3 and 1.3 Ga in all studied area (Fig. 9).

An alternative mechanism is a change in the major granitoid formation process. There are prominent geochemical differences between typical Archean granitoids (TTG: tonalite–trondhjemite–granodiorite) and most post-Archean granitoids which follow a calc-alkaline differentiation trend, particularly with regard to REE patterns: the former show HREE depletion and no Eu anomalies, while the latter have negative Eu anomalies. Based on this, the style of major granitoid genesis has been considered to change from the Archean to the Proterozoic as a consequence of the cooling of Earth. In the Archean, granitoid magmas were generated at depths in equilibrium with residual garnet (Petford and Atherton, 1996; Smithies, 2000; Whalen et al., 2002; Rapp et al., 2003; Condie, 2008) probably by partial melting of young subducted crust (Martin, 1986; Drummond and Defant, 1990; Foley et al., 2002; Hiess et al., 2009), whereas during post-Archean times most granitoid magmas formed at crustal depths in the presence of plagioclase as a residual or fractionating phase (Wyllie, 1984; Taylor and McLennan, 1985). Indeed, our data show that the median Eu/Eu* values of zircons from the Amazon River decrease during the Paleoproterozoic era (Fig. 8h), while for the other studied rivers the values of Archean post-Archean zircons overlap within internal quartiles (Fig. 8e–g). The Eu/Eu* secular change might reflect that granitoid magma genesis by crustal melting became increasingly more important during the Paleoproterozoic era. However, the observed secular trends in the reworking index are opposite of that expected. In addition, the lack of correlation between εHf(t) and Eu/Eu* (Fig. 11) as well as other geochemical parameters does not support this interpretation. We therefore consider that a variation in rate of continental crust generation is more likely to account for the secular changes in the reworking index than the transition of the style of major granitoid genesis.

5.5. Implications for episodic continental crust generation

While rocks amendable to study on the continental surface are generally not a direct sample of newly generated crust, the timing of possible episodic crust generation has been proposed based on the following two observations. The first is that radiogenic isotope (Sr, Nd, Hf) model ages of granitoids and sediments cluster around 3.6, 3.3, 2.7,

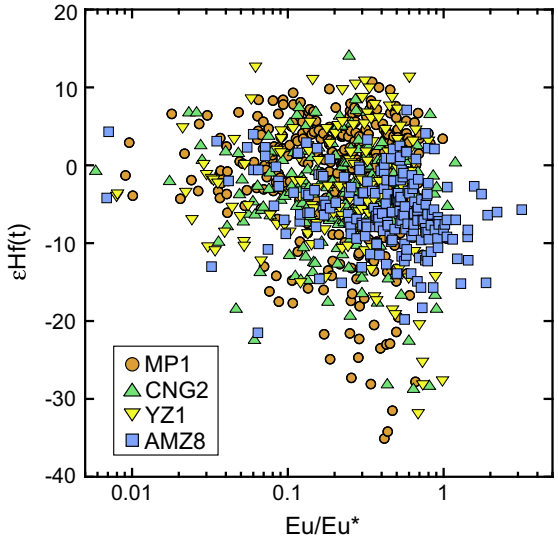

Fig. 11. Plot of εHf(t) versus Eu/Eu* for detrital zircons from sample of this study.

1.9, 1.2, and/or 0.5 Ga (Nelson and DePaolo, 1985; Patchett and Arndt, 1986; McCulloch and Bennett, 1994; Jahn, 2004; Kemp et al., 2006; Yang et al., 2009; Wang et al., 2009). The T_{DM} population of our detrital zircons (Fig. 7b) is consistent with these results. However, as previously mentioned (Section 5.2), the model age peaks could reflect hybrid ages of multi-juvenile crust formation events (Arndt and Goldstein, 1987). The second observation is that the zircon U–Pb ages of isotopically juvenile granitoids on different continents show peaks around 2.7, 2.1, 1.9, and 1.2 Ga (Boher et al., 1992; Condie, 1998; O'Reilly et al., 2008). The 'hybrid age' problem can be largely circumvented by this method. Note, however, that our data reveal that the isotopically juvenile granitoids are minor in the upper continental crust. Thus, juvenile granitoid record alone might be highly incomplete and insufficient to investigate the growth history of continental crust. More recently, it has been shown that Os isotopic model ages of ophiolite and mantle xenolith samples also cluster around 3.3–2.5, 1.9, and 1.2 Ga, possibly reflecting significant mantle depletion by episodic crust generation at these times (e.g., Griffin et al., 2003; Carlson and Pearson, 2005; Pearson et al., 2007).

Given that the reworking index in granitoid crust formation depends on the rate of continental crust generation, the temporal variations of the reworking index, based on a significant number of detrital zircon U–Pb and Lu–Hf data, can be used to evaluate models for episodic generation of the continental crust. Our results indicate that the rate of continental crust generation increased around (or before) 3.3 and 1.3 Ga in all studied areas (Fig. 9). The high rates of crust generation around 2.7 and 1.9 Ga, that have been proposed by Condie (1998), are defined in the detrital zircon record of some of the studied rivers (the Yangtze and Congo Rivers for circa 2.7 Ga event and the Mississippi and Amazon Rivers for circa 1.9 Ga event, respectively). Our results also indicate that crust generation was relatively minor, and crustal differentiation was the dominant feature of the evolution of continental crust at 2.3–2.2 Ga and after 0.6 Ga in all studied areas. While further zircon U–Pb and Lu–Hf isotopic work on other major rivers is clearly required to evaluate the generality of the conclusions, our current pictures clearly support the model for the episodic global generation of the continental crust.

Despite of the potential 'hybrid age' problem in model age calculation, the observed peaks in the model age population (Fig. 7b) do in fact broadly correspond with the juvenile granitoid age population (Condie, 1998) and also with the timing of low reworking index in granitoid crust formation (Fig. 9). This association may suggest that in many granitoid magmas, a crustal component dominates over a juvenile mantle component, and therefore that the model ages approximate the timing of juvenile crust formation events. The implication of this interpretation is that even restricted addition of juvenile magmas to the continental crust can cause significant intra-crustal melting.

6. SEDIMENTARY GROWTH AND RECYCLING

Sediments are major components of crustal materials recycled into the mantle, and therefore potentially modify the composition of the mantle. Sedimentary systems also control the composition of the ocean and the atmosphere through weathering, erosion and deposition processes (e.g., Veizer and Compston, 1976; Kramers, 2002; Lowe and Tice, 2004). Hence, knowledge of sedimentary dynamics is essential to better understanding the evolution of the Earth's crust-mantle and surface environment. The temporal Hf isotopic evolution of granitoid crust identified here can provide new insights into the growth and recycling of the sedimentary mass by combining with the Nd and Hf isotopic data of sedimentary rocks.

The Nd and Hf model ages of sedimentary rocks reflect the mean mantle-extraction age of the various provenance components. Fig. 12a summarizes the Nd and Hf isotopic data from sedimentary rocks as plots of the sedimentation age versus the Nd or Hf model age (from data compilation in McLennan and Hemming, 1992; Vervoort et al., 1999). It illustrates that for most sedimentary rocks the model age exceeds the sedimentation age and that the age difference generally increases from ~2.5 Ga to the present. Two interpretations of these data have been made. The first (O'Nions et al., 1983; Allègre and Rousseau, 1984) interpreted that sediments are primarily representative samples of the crystalline crusts feeding the sedimentary basins and the Nd isotopic data reflect the crustal residence time of the continental crust. It is, however, well established that the rate of sedimentary recycling is much faster than the erosion of old igneous basement (Veizer and Jansen, 1979, 1985; Goldstein et al., 1984; Michard et al., 1985; McLennan, 1988; Veizer and Mackenzie, 2003). Therefore, alternatives (Veizer and Jansen, 1985; Mclennan, 1988; McLennan and Hemming, 1992) consider that the Nd isotopic data reflect growth and recycling of sedimentary system. Assuming that the effect of crustal reworking is insignificant relative to that of sedimentary recycling, the age difference has been interpreted in terms of the relative importance of the cannibalistic sedimentary recycling versus first-cycling of the young igneous basement having a short crustal residence time. This has led to the inference that the sedimentary mass grew to a near present-day sedimentary mass through addition of first-cycle sediments from young igneous basements, until after ~2.5 Ga when cannibalistic recycling became dominant. However, our results (Fig. 6) clearly indicate that crustal reworking is an important process in granitoid crust formation, and therefore that the igneous precursors of sediments should have long crustal residence times, calling for re-evaluation in sedimentary evolutionary models.

To distinguish the effects of sedimentary recycling and crustal reworking, the model ages of sedimentary rocks are compared with the mean Hf model ages of the contemporaneous granitoid crusts (Fig. 12b and c). The mean Hf model ages of granitoid crusts are calculated from the mean values of the $\varepsilon Hf(t)$ medians for zircons from the large rivers and from sedimentary rocks (Fig. 6f and Table 4). Because sediments in active margins (Fig. 12b) and continental (cratonic/passive) settings (Fig. 12c) have systematically different model ages (McLennan and Hemming, 1992; Vervoort et al., 1999), we evaluate the two groups of sediments separately. Two remarkable features are evident.

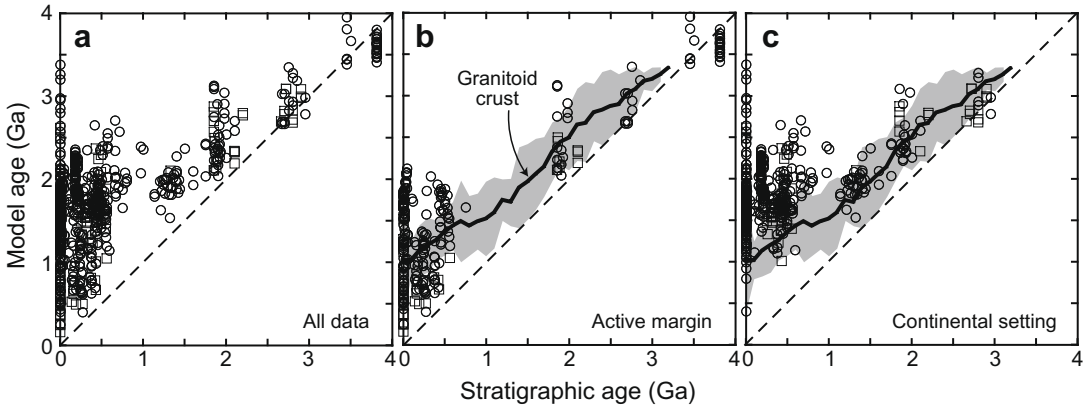

Fig. 12. Reconciling the igneous and sedimentary records. Plots of Hf (squares) or Nd (circles) model age versus stratigraphic age (a) for all sediments (from data compilation in McLennan and Hemming, 1992, and Vervoort et al., 1999), (b) sediments deposited in active margins, and (c) sediments deposited in continental settings. The data from Vervoort et al. (1999) were recalculated using the ^{176}Lu decay constant of 1.867×10^{-11}, and the parameters of the depleted mantle defined in this study. The mean T_{DM} (solid line) $\pm$ 2 s.d. (shaded area) of the contemporaneous granitoid crusts, calculated from averaged T_{DM} for zircons from the large rivers and passive margin sedimentary rocks (Fig. 6f and Table 4), are also shown as a function of the crystallization age.

First, active margin sediments have, on average, similar model ages to those of the contemporaneous granitoid crusts through geological history, while the model ages of young continental samples markedly exceed those of the granitoid crusts. This indicates that sedimentary recycling has primarily taken place in continental settings rather than tectonically active margin settings. Minor recycling at active margins can be explained by efficient sediment loss from the system by subduction and/or accretion to the deep crust (Reymer and Schubert, 1984; Hay et al., 1988; von Huene and Scholl, 1993; Rea and Ruff, 1996; Plank and Langmuir, 1998; Clift and Hartley, 2007). The major control by tectonic setting on sedimentary recycling rate has been also demonstrated by Veizer and Jansen (1985) which examined the mass-age relationship in modern various tectonic sediments and demonstrated that the half-life of continental sediments is >10 times longer than that of active margin sediments, consistent with our results.

Second, the excess of model ages of continental sedimentary rocks over the granitoid crusts is rarely observed in samples older than ~1.5 Ga. This is best explained if the continental sedimentary mass was growing significantly by the addition of first-cycle sediments from contemporaneous igneous precursors until ~1.5 Ga, and subsequently cannibalistic recycling became the dominant feature of sedimentary evolution. This interpretation is consistent with the observed secular change in Th/U of sedimentary rocks. Under oxidizing conditions, U^{4+} is oxidized to U^{6+} which is highly soluble and readily mobilized during rock weathering, whereas Th^{4+} does not change oxidation state and remains insoluble during weathering. Hence, if sedimentary recycling is important in sedimentary evolution, it should be accompanied by an increase in Th/U, as multi-cycled components should preferentially lose U. Indeed, sedimentary rocks younger than 1.5 Ga have high Th/U relative to those older than 1.5 Ga (McLennan and Taylor, 1980; Taylor and McLennan, 1985). In addition, because the size of the continental sedimentary mass is principally a function of the extent of the continents (Veizer and Jansen, 1985), our inference for sedimentary growth is compatible with the variation in rate of continental crust generation to explain the observed $\varepsilon Hf(t)$ trends in the granitoid crusts (see Sections 5.4 and 5.5).

A relevant question in sedimentary evolution is: When did the accumulation of sedimentary masses begin so that they could be recycled into younger sediments? The oldest of detrital zircons from large rivers generally have U–Pb ages of circa 3.3 Ga (Fig. 7a; Campbell and Allen, 2008; Rino et al., 2008). Given that detrital zircons in river sands and sedimentary rocks were essentially derived from older sedimentary rocks and young contemporaneous igneous basements (Rahl et al., 2003; Campbell et al., 2005; see also Section 4), the observation suggests that sedimentary recycling was generally operative by around 3.3 Ga. On the other hand, the oldest zircon Hf model ages for the river sands are circa 3.7 Ga (Fig. 7b). The lack of >3.3 Ga zircons, despite the zircon Hf model ages up to 3.7 Ga, could be interpreted to indicate that Eo- and Paleoarchaean crusts dominantly comprise mafic rocks, which contain few magmatic zircon (Vervoort and Blichert-Toft, 1999; Foley et al., 2003). We consider this unlikely, however, because granitoid formation process under the presence of liquid water oceans appear to be established by 4.2 Ga (e.g., Cavosie et al., 2005; Watson and Harrison, 2005; Ushikubo et al., 2008; Harrison, 2009). Indeed, preserved Eo- and Paleoarchaean terranes generally exhibit bimodal occurrences of mafic (greenstone) and granitoid (TTG) rocks (de Wit and Hart, 1993; Windley, 1995). An alternative and more plausible explanation is that certain amounts of granitoid crust were formed and eroded to be deposited in sediments, but at that time the first-cycle sediments were efficiently removed from sedimentary recycling system via subduction into the mantle and/or accretion to the deep crust. This view is consistent with the paucity of Eo- and Paleoarchean mature sedimentary rocks such as quartz-rich sandstones (Lowe, 1994; Veizer and Mackenzie, 2003; Valley et al., 2005). Because sedimentary recycling has primarily taken place in continental settings rather than tectonically active margin

settings, these observations may indicate that crusts generated during Eo- and Paleoarchaean time formed island arcs, and that sediment accumulation accompanied by sedimentary recycling generally began at around 3.3 Ga, as a result of the stabilization of a critical volume of crust that permitted the establishment of continental basins or shelves (Flament et al., 2008). This inference is consistent with geological evidence for the oldest continental block having formed at circa 3.4 Ga (Buick et al., 1995).

Presumably, the hotter and, therefore, rheologically weaker lithospheric mantle fostered many small plates and island arcs early in Earth's history (Dewey and Windley, 1981; Richter, 1988; Takahashi, 1990; Nisbet et al., 1993; de Wit and Hart, 1993; Komiya, 2004; Berry et al., 2008; Rey and Coltice, 2008), and the young arc crust was efficiently returned to the mantle via subduction. Accordingly, net growth of continental crust was essentially minor in early Earth's history despite high rates of crust generation. The formation of the continents was delayed until a time when moderately strong and large plates were formed and newly formed crust was able to survive through collision amalgamation and sediment accumulation accompanied by sedimentary recycling in passive tectonic settings (Dewey and Windley, 1981; de Wit and Hart, 1993).

Overall, the lines of evidence from detrital zircons imply that generation of continental crust began by 3.7 Ga and continued over geological time with major global increases around (or before) 3.3 and 1.3 Ga. This process, in conjunction with the secular cooling and strengthening of the lithospheric mantle, resulted in the emergence of the continents around 3.3 Ga with further rapid growth around 1.3 Ga. The continental crust development led to the major growth of the sedimentary mass between 3.3 and 1.3 Ga, and the predominance of its cannibalistic recycling later.

ACKNOWLEDGMENTS

We thank N. Hammond, I. Katayama, F. Makoka, and A. Motoki for assistance in fieldwork, K. Hamano for assistance in data reduction, and F. Albarède, J. Blichert-Toft, S. Johnson, M. McCulloch, J. Vervoort, and B. Windley for reading early versions of the manuscript and constructive comments. Critical reviews by K. Condie, W. Griffin, and J. Hiess improved the manuscript and the editorial handling of A. Brandon is acknowledged. This work was financed by grants from the Ministry of Education, Culture, Sports, Technology and Science, Japan. T.I. thanks the Research Fellowships of the Japan Society for the Promotion of Science.

APPENDIX A. SUPPLEMENTARY DATA

Supplementary data associated with this article can be found, in the online version, at doi:10.1016/j.gca.2010.01.023.

REFERENCES

Albarède F. (1998) The growth of continental crust. *Tectonophysics* **296**, 1–14.

Allègre C. J. and Ben Othman D. (1980) Nd–Sr isotopic relationship in granitoid rocks and continental crust development – a chemical approach to orogenesis. *Nature* **286**, 335–342.

Allègre C. J. and Rousseau D. (1984) The growth of the continent through geological time studied by Nd isotope analysis of shales. *Earth Planet. Sci. Lett.* **67**, 19–34.

Amelin Y., Lee D.-C., Halliday A. N. and Pidgeon R. T. . (1999) Nature of the Earth's earliest crust from hafnium isotopes in single detrital zircons. *Nature* **399**, 252–255.

Amelin Y., Lee D.-C. and Halliday A. N. (2000) Early-middle Archaean crustal evolution deduced from Lu–Hf and U–Pb isotopic studies of single zircon grains. *Geochim. Cosmochim. Acta* **64**, 4205–4225.

Amidon W. H., Burbank D. W. and Gehrels G. E. (2005) U–Pb zircon ages as a sediment mixing tracer in the Nepal Himalaya. *Earth Planet. Sci. Lett.* **235**, 244–260.

Annen C., Blundy J. D. and Sparks R. S. J. (2006) The genesis of intermediate and silicic magmas in deep crustal hot zones. *J. Petrol.* **47**, 505–539.

Armstrong R. L. (1981) Radiogenic isotopes: the case for crustal recycling on a near-steady state no-continental-growth Earth. *Philos. Trans. R. Soc. Lond. A* **301**, 443–472.

Arndt N. T. and Goldstein S. L. (1987) Use and abuse of crust-formation ages. *Geology* **15**, 893–895.

Balan E., Trocellier P., Jupille J., Fritsch E., Muller J. P. and Calas G. (2001) Surface chemistry of weathered zircons. *Chem. Geol.* **181**, 13–22.

Belousova E. A., Griffin W. L., O'Reilly S. Y. and Fisher N. I. (2002) Igneous zircon: trace element composition as an indicator of source rock type. *Contrib. Mineral. Petrol.* **143**, 602–622.

Berry A. J., Danyushevsky L. V., O'Neill H. St. C., Newville M. and Sutton S. R. (2008) Oxidation state of iron in komatiitic melt inclusions indicates hot Archaean mantle. *Nature* **455**, 960–963.

Bleeker W. (2003) The late Archean record: a puzzle in ca. 35 pieces. *Lithos* **71**, 99–134.

Blichert-Toft J. (2008) The Hf isotopic composition of zircon reference material 91500. *Chem. Geol.* **253**, 252–257.

Blichert-Toft J. and Albarède F. (2008) Hafnium isotopes in Jack Hills zircons and the formation of the Hadean crust. *Earth Planet. Sci. Lett.* **265**, 686–702.

Blichert-Toft J., Albarède F., Rosing M., Frei R. and Bridgwater D. (1999) The Nd and Hf isotopic evolution of the mantle through the Archean. Results from the Isua supracrustals, West Greenland, and from the Birimian terranes of West Africa. *Geochim. Cosmochim. Acta* **63**, 3901–3914.

Bodet F. and Schärer U. (2000) Evolution of the SE-Asian continent from U–Pb and Hf isotopes in single grains of zircon and baddeleyite from large rivers. *Geochim. Cosmochim. Acta* **64**, 2067–2091.

Boher M., Abouchami W., Michard A., Albarède F. and Arndt N. T. (1992) Crustal Growth in West Africa at 2.1 Ga. *J. Geophys. Res.* **97**, 345–369.

Bouvier A., Vervoort J. D. and Patchett P. J. (2008) The Lu–Hf and Sm–Nd isotopic composition of CHUR: constraints from unequilibrated chondrites and implications for the bulk composition of terrestrial planets. *Earth Planet. Sci. Lett.* **273**, 48–57.

Bowring S. A. and Housh T. B. (1995) The Earth's early evolution. *Science* **269**, 1535–1540.

Buick R., Thornett N. J., McNaugh N. J., Smith J. B., Barley M. E. and Savage M. (1995) Record of emergent continental crust ~3.5 billion years ago in the Pilbara craton of Australia. *Nature* **375**, 574–577.

Campbell I. H. and Allen C. A. (2008) Formation of supercontinents linked to increases in atmospheric oxygen. *Nature Geosci.* **1**, 554–558.

Campbell I. H. and Taylor S. R. (1983) No water, no granites – no oceans, no continents. *Geophys. Res. Lett.* **10**, 1061–1064.

Campbell I. H., Reiners P. W., Allen C. M., Nicolescu S. and Upadhyay R. (2005) He–Pb double dating of detrital zircons from the Ganges and Indus Rivers: implication for quantifying sediment recycling and provenance studies. *Earth Planet. Sci. Lett.* **237**, 402–432.

Carlson R. W. and Pearson D. G. (2005) Physical, chemical, and gechronological characteristics of continental mantle. *Rev. Geophys.* **43**, 2004RG000156.

Carter A. and Bristow C. S. (2000) Linking hinterland evolution and continental basin sedimentation by using detrital zircon thermochronology: a study of the Khorat Plateau Basin, eastern Thailand. *Basin Res.* **15**, 271–285.

Carter A. and Moss S. J. (1999) Combined detrital-zircon fission-track and U–Pb dating: a new approach to understanding hinterland evolution. *Geology* **27**, 235–238.

Cavosie A. J., Valley J. W., Wilde S. A. and EIMF (2005) Magmatic $\delta^{18}O$ in 4400–3900 Ma detrital zircons: a record of the alteration and recycling of crust in the Early Archean. *Earth Planet. Sci. Lett.* **235**, 663–681.

Cawood P. A. and Buchan C. (2007) Linking accretionary orogenesis with supercontinent assembly. *Earth Sci. Rev.* **82**, 217–256.

Chappell B. W. (1984) Source rocks of I- and S-type granites in the Lachlan Fold Belt, southeastern Australia. *Philos. Trans. R. Soc. Lond. A* **310**, 693–707.

Cherniak D. J. and Watson E. B. (2001) Pb diffusion in zircon. *Chem. Geol.* **172**, 5–24.

Christensen N. I. and Mooney W. D. (1995) Seismic velocity structure and composition of the continental crust: a global review. *J. Geophys. Res.* **100**, 9761–9788.

Chu N. C., Taylor R. N., Chavagnac V., Nesbitt R. W., Boella M., Milton J. A., German C. R., Bayon G. and Burton K. (2002) Hf isotope ratio analysis using multi-collector inductively coupled plasma mass spectrometry: an evaluation of isobaric interference corrections. *J. Anal. Atom. Spectrom.* **17**, 1567–1574.

Clift P. D. and Hartley A. J. (2007) Slow rates of subduction erosion and coastal underplating along the Andean margin of Chile and Peru. *Geology* **35**, 503–506.

Condie K. C. (1998) Episodic continental growth and supercontinents: a mantle avalanche connection? *Earth Planet. Sci. Lett.* **163**, 97–108.

Condie K. C. (2008) Did the character of subduction change at the end of the Archean? Constraints from convergent-margin granitoids. *Geology* **36**, 611–614.

Condie K. C., Beyer E., Belousova E., Griffin W. L. and O'Reilley S. Y. (2005) U–Pb isotopic ages and Hf isotopic composition of single zircons: the search for juvenile Precambrian continental crust. *Precambrian Res.* **139**, 42–100.

Condie K. C., O'Neill C. and Aster R. C. (2009) Evidence and implications for a widespread magmatic shutdown for 250 My on Earth. *Earth Planet. Sci. Lett.* **282**, 294–298.

Corfu F. (2007) Comment to short-communicatioin 'Comment: Hf-isotope heterogeneity in zircon 91500' by W.L. Griffin, N.J. Pearson, E.A. Belousova and A. Saeed (Chemical Geology 233 (2006) 358–363). *Chem. Geol.* **244**, 350–353.

Dalziel I. W. D., Mosher S. and Gahagan L. M. (2000) Laurentia-Kalahari collision and the assembly of Rodinia. *J. Geol.* **108**, 499–513.

Davies G. F. (2008) Episodic layering of the early mantle by the 'basalt barrier' mechanism. *Earth Planet. Sci. Lett.* **275**, 382–392.

Davis D. W., Amelin Y., Nowell G. M. and Parrish R. R. (2005) Hf isotopes in zircon from the western Superior province, Canada: implications for Archean crustal development and evolution of the depleted mantle reservoir. *Precambrian Res.* **140**, 132–156.

De Waele B., Johnson S. P. and Pisarevsky S. A. (2008) Paleoproterozoic to Neoproterozoic growth and evolution of the eastern Congo Craton: its role in the Rodinia puzzle. *Precambrian Res.* **160**, 127–141.

de Wit M. J. and Hart R. A. (1993) Earth's earliest continental lithosphere, hydrothermal flux and crustal recycling. *Lithos* **30**, 309–335.

Deniel C., Vidal P., Fernandez A., Le Fort A. and Peucat J. J. (1987) Isotopic study of the Manasulu granite (Himalaya Nepal): inferences on the age and source of Himalayan leucogranites. *Contrib. Mineral. Petrol.* **96**, 78–92.

DePaolo D. J. (1981) Neodymium isotopes in the Colorado Front Range and implications for crust formation and mantle evolution in the Proterozoic. *Nature* **291**, 193–197.

DePaolo D. J. and Wasserburg G. J. (1976) Nd isotopic variations and petrogenic models. *Geophys. Res. Lett.* **3**, 249–252.

Dewey J. F. and Windley B. F. (1981) Growth and differentiation of the continental crust. *Philos. Trans. R. Soc. Lond. A* **301**, 189–206.

Dosseto A., Bourdon B., Gaillardet J., Allègre C. J. and Filizola N. (2006) Time scale and conditions of weathering under tropical climate: study of the Amazon basin with U-series. *Geochim. Cosmochim. Acta* **70**, 71–89.

Drummond M. S. and Defant M. J. (1990) A model for trondhjemite-tonalite-dacite genesis and crustal growth via slab melting – Archean to modern comparisons. *J. Geophys. Res.* **95**, 21503–21521.

Flament N., Coltice N. and Rey P. F. (2008) A case for late-Archaean continental emergence from thermal evolution models and hypsometry. *Earth Planet. Sci. Lett.* **275**, 326–336.

Foley S., Tiepolo M. and Vannucci R. (2002) Growth of early continental crust controlled by melting of amphibolite in subduction zones. *Nature* **417**, 837–840.

Foley S. F., Buhre S. and Jacob D. E. (2003) Evolution of the Archaean crust by delamination and shallow subduction. *Nature* **421**, 249–252.

France-Lanord C. and Le Fort P. (1988) Crustal melting and granite genesis during the Himalayan collision orogenesis. *Trans. R. Soc. Edinburg: Earth Sci.* **79**, 183–195.

Fyfe W. S. (1978) The evolution of the Earth crust: modern plate tectonics to ancient hot spot tectonics? *Chem. Geol.* **23**, 89–114.

Gao S., Luo T. C., Zhang B. R., Zhang H. F., Han Y. W., Zhao Z. D. and Hu Y. K. (1998) Chemical composition of the continental crust as revealed by studies in East China. *Geochim. Cosmochim. Acta* **62**, 1959–1975.

Gastil G. (1960) The distribution of mineral dates in time and space. *Am. J. Sci.* **258**, 1–35.

Gerdes A. and Zeh A. (2006) Combined U–Pb and Hf isotope LA-(MC-)ICP-MS analyses of detrital zircons: comparison with SHRIMP and new constraints for the provenance and age of an Annorican metasediment in Central Germany. *Earth Planet. Sci. Lett.* **249**, 47–61.

Gerdes A. and Zeh A. (2009) Zircon formation versus zircon alteration – new insights from combined U–Pb and Lu–Hf in-situ LA-ICP-MS analyses, and consequences for the interpretation of Archean zircon from the Central Zone of the Limpopo Bet. *Chem. Geol.* **261**, 230–243.

Goldstein S. L., Onions R. K. and Hamilton P. J. (1984) A Sm–Nd isotopic study of atmospheric dusts and particulates from major river systems. *Earth Planet. Sci. Lett.* **70**, 221–236.

Goldstein S. L., Arndt N. T. and Stallard R. F. (1997) The history of a continent from U–Pb ages of zircons from Orinoco River sand and Sm–Nd isotopes in Orinoco basin river. *Chem. Geol.* **139**, 271–286.

Griffin W. L., Pearson N. J., Belousova E., Jackson S. E., van Achterbergh E. and O'Reilly S. (2000) The Hf isotope compo-

sition of cratonic mantle: LAM-MC-ICPMS analysis of zircon megacrysts in kimberlites. *Geochim. Cosmochim. Acta* **64**, 133–147.

Griffin W. L., O'Reilly S. Y., Abe N., Aulbach S., Davies R. M., Pearson N. J., Doyle B. J. and Kivi K. (2003) The origin and evolution of Archean lithospheric mantle. *Precambrian Res.* **127**, 19–41.

Griffin W. L., Pearson N. J., Belousova E. A. and Saeed A. (2006) Comment: Hf-isotope heterogeneity in zircon 91500. *Chem. Geol.* **233**, 358–363.

Griffin W. L., Pearson N. J., Belousova E. A. and Saeed A. (2007) Reply to "Comment to short-communication "Comment: Hf-isotope heterogeneity in zircon 91500' by W.L. Griffin, N.J. Pearson, E.A. Belousova and A. Saeed (Chemical Geology 233 (2006) 358–363)" by F. Corfu. *Chem. Geol.* **244**, 354–356.

Grove T. L., DonnellyNolan J. M. and Housh T. (1997) Magmatic processes that generated the rhyolite of Glass Mountain, Medicine Lake volcano, N California. *Contrib. Mineral. Petrol.* **127**, 205–223.

Harmon R. S., Barreiro B. A., Moorbath S., Hoefs J., Francis P. W., Thorpe R. S., Deruelle B., Mchugh J. and Viglino J. A. (1984) Regional O isotope, Sr isotope, and Pb isotope relationships in Late Cenozoic calc-alkaline lavas of the Andean Cordillera. *J. Geol. Soc.* **141**, 803–822.

Harrison T. M. (2009) The Hadean crust: evidence from >4 Ga zircon. *Annu. Rev. Earth Sci.* **37**, 479–505.

Harrison T. M., Schmitt A. K., McCulloch M. T. and Lovera O. M. (2008) Early ($\geqslant$4.5 Ga) formation of terrestrial crust: Lu–Hf, $\delta^{18}O$, and Ti thermometry results for Hadean zircons. *Earth Planet. Sci. Lett.* **268**, 476–486.

Hawkesworth C. J. and Kemp A. I. S. (2006) Evolution of the continental crust. *Nature* **443**, 811–817.

Hay W. W., Sloan J. L. and Wold C. N. (1988) Mass age distribution and composition of sediments on the ocean-floor and the global rate of sediment subduction. *J. Geophys. Res.* **93**, 14933–14940.

Hiess J., Bennett V. C., Nutman A. P. and Williams I. S. (2009) In situ U–Pb, O and Hf isotopic compositions of zircon and olivine from Eoarchaean rocks, West Greenland: new insights into making old crust. *Geochim. Cosmochim. Acta* **73**, 4489–4516.

Hill R. I. (1993) Mantle plumes and continental tectonics. *Lithos* **30**, 193–206.

Hirata T. and Nesbitt R. W. (1995) U–Pb isotopic geochronology of zircon: evaluation of the laser probe-inductively coupled plasma mass spectrometry technique. *Geochim. Cosmochim. Acta* **59**, 2491–2500.

Hirata T., Iizuka T. and Orihashi Y. (2005) Reduction of mercury background on ICP-mass spectrometry for in situ U–Pb age determinations of zircon samples. *J. Anal. Atom. Spectrom.* **20**, 696–701.

Hoskin P. W. O. and Black L. P. (2000) Metamorphic zircon formation by solid-state recrystallization of protolith igneous zircon. *J. Metamorph. Geol.* **18**, 423–439.

Hoskin P. W. O. and Ireland T. R. (2000) Rare earth element chemistry of zircon and its use as a provenance indicator. *Geology* **28**, 627–630.

Hurley P. M. and Rand J. R. (1969) Pre-drift continental nuclei. *Science* **164**, 1229–1242.

Iizuka T. and Hirata T. (2004) Simultaneous determinations of U–Pb age and REE abundances for zircons using ArF excimer laser ablation-ICPMS. *Geochem. J.* **38**, 229–241.

Iizuka T. and Hirata T. (2005) Improvements of precision and accuracy in in situ Hf isotope microanalysis of zircon using the laser ablation-MC-ICPMS technique. *Chem. Geol.* **220**, 121–137.

Iizuka T., Hirata T., Komiya T., Rino S., Katayama I., Motoki A. and Maruyama S. (2005) U–Pb and Lu–Hf isotope systematics of zircons from the Mississippi River sand: Implications for reworking and growth of continental crust. *Geology* **33**, 485–488.

Iizuka T., Komiya T., Johnson S. P., Kon Y., Maruyama S. and Hirata T. (2009) Reworking of Hadean crust in the Acasta gneisses, northwestern Canada: Evidence from in-situ Lu–Hf isotope analysis of zircon. *Chem. Geol.* **259**, 230–239.

Inger S. and Harris N. (1993) Geochemical constraints on leucogranite magmatism in the Langtang valley, Nepal Himalaya. *J. Petrol.* **34**, 345–368.

Jagoutz O. E., Burg J.-P., Hussain S., Dawood H., Pettke T., Iizuka T. and Maruyama S. (2009) Construction of the granitoid crust of an island arc part I: geochronological and geochemical constraints from the plutonic Kohistan (NW Pakistan). *Contrib. Mineral. Petrol.* **158**, 739–755.

Jahn B. M. (2004) The central Asian Orogenic Belt and growth of the continental crust in the Phanerozoic. *Geol. Soc. Spec. Publ.* **226**, 73–100.

Johnson C. M. and Beard B. L. (1993) Evidence from hafnium isotopes for ancient sub-oceanic mantle beneath the Rio-Grande Rift. *Nature* **362**, 441–444.

Johnson S. P., Rivers T. and De Waele B. (2005) A review for the Mesoproterozoic to early Proterozoic magmatic and tectonothermal history of south–central Africa: implications for Rodinia and Gondwana. *J. Geol. Soc. Lond.* **162**, 433–450.

Kemp A. I. S., Hawkesworth C. J., Paterson B. A. and Kinny P. D. (2006) Episodic growth of the Gondwana supercontinent from hafnium and oxygen isotopes in zircon. *Nature* **439**, 580–583.

Kemp A. I. S., Hawkesworth C. J., Foster G. L., Paterson B. A., Woodhead J. D., Hergt J. M., Gray C. M. and Whitehouse M. J. (2007) Magmatic and crustal differentiation history of granitic rocks from Hf–O isotopes in zircon. *Science* **315**, 980–983.

Komiya T. (2004) Material circulation model including chemical differentiation within the mantle and secular variation of temperature and composition of the mantle. *Phys. Earth Planet. Int.* **146**, 333–367.

Kramers J. D. (2002) Global modeling of continent formation and destruction through geological time and implications for CO_2 drawdown in the Archaean Eon. *Geol. Soc. Spec. Publ.* **199**, 259–274.

Ledent D., Patterson C. and Triton G. R. (1964) Ages of zircon and feldspar concentrates from Northern American beach sand. *J. Geol.* **72**, 112–122.

Lee J. K. W., Williams I. S. and Ellis D. J. (1997) Pb, U and Th diffusion in natural zircon. *Nature* **390**, 159–162.

Lowe D. R. (1994) Archean greenstone-related sedimentary rocks. In *Archean Crustal Evolution* (ed. K. C. Condie). Elsevier, pp. 121–169.

Lowe D. R. and Tice M. M. (2004) Geologic evidence for Archean atmospheric and climatic evolution: fluctuating levels of CO_2, CH_4, and O_2, with an overriding tectonic control. *Geology* **32**, 493–496.

Martin H. (1986) Effects of steeper Archean geothermal gradient on geochemistry of subduction-zones magmas. *Geology* **14**, 753–756.

McCulloch M. T. and Bennett V. C. (1994) Progressive growth of the Earth's continental crust and depleted mantle: geochemical constraints. *Geochim. Cosmochim. Acta* **58**, 4717–4738.

McLennan S. M. (1988) Recycling of the continental crust. *Pure Appl. Geophys.* **128**, 683–724.

McLennan S. M. and Hemming S. (1992) Samarium neodymium elemental and isotopic systematics in sedimentary rocks. *Geochim. Cosmochim. Acta* **56**, 887–898.

McLennan S. M. and Taylor S. R. (1980) Th and U in sedimentary rocks – crustal evolution and sedimentary recycling. *Nature* **285**, 621–624.

Michard A., Gurriet P., Soudant M. and Albarède F. (1985) Nd isotopes in French Phanerozoic shales – external vs internal aspects of crustal evolution. *Geochim. Cosmochim. Acta* **49**, 601–610.

Milliman J. D. and Syvitski J. P. M. (1992) Geomorphic tectonic control of sediment discharge to the ocean – the importance of small mountainous rivers. *J. Geol.* **100**, 525–544.

Moorbath S. (1978) Age and isotope evidence for evolution of continental crust. *Philos. Trans. R. Soc. Lond. A* **288**, 401–412.

Nebel-Jacobsen Y., Scherer E. E., Münker C. and Mezger K. (2005) Separation of U, Pb, Lu, and Hf from single zircons for combined U–Pb dating and Hf isotope measurements by TIMS and MC-ICPMS. *Chem. Geol.* **220**, 105–120.

Nebel O., Nebel-Jacobsen Y., Mezger K. and Berndt J. (2007) Initial Hf isotope compositions in magmatic zircon from early Proterozoic rocks from the Gawler Craton, Australia: A test for zircon model ages. *Chem. Geol.* **241**, 27–37.

Nelson B. K. and DePaolo D. J. (1985) Rapid production of continental crust 1.7–1.9 b.y. ago; Nd isotopic evidence from the basement of the North American mid-continent. *Geol. Soc. Am. Bull.* **96**, 746–754.

Nisbet E. G., Cheadle M. J., Arndt N. T. and Bickle M. J. (1993) Constraining the potential temperature of the Archean mantle: a review of the evidence from komatiites. *Lithos* **30**, 291–307.

Nowell G. M., Kempton P. D., Noble S. R., Fitton J. G., Saunders A. D., Mahoney J. J. and Taylor R. N. (1998) High precision Hf isotope measurements of MORB and OIB by thermal ionisation mass spectrometry: insights into the depleted mantle. *Chem. Geol.* **149**, 211–233.

O'Nions R. K., Hamilton P. J. and Hooker P. J. (1983) A Nd isotope investigation of sediments related to crustal development in the British-Isles. *Earth Planet. Sci. Lett.* **63**, 229–240.

O'Reilly S. Y., Griffin W. L., Pearson N. J., Jackson S. E., Belousova E. A., Alard O. and Saeed A. (2008) Taking the pulse of the Earth: linking crustal and mantle events. *Aust. J. Earth Sci.* **55**, 983–995.

Patchett P. J. and Arndt N. T. (1986) Nd isotopes and tectonics of 1.9–1.7 Ga crustal genesis. *Earth Planet. Sci. Lett.* **78**, 329–338.

Patchett P. J., Kouvo O., Hedge C. E. and Tatsumoto M. (1981) Evolution of continental crust and mantle heterogeneity: evidence from Hf isotopes. *Contrib. Mineral. Petrol.* **78**, 279–297.

Patchett P. J., White W. M., Feldmann H., Kielinczuk S. and Hofmann A. W. (1984) Hafnium rare-Earth element fractionation in the sedimentary system and crustal recycling into the Earth's mantle. *Earth Planet. Sci. Lett.* **69**, 365–378.

Pearson D. G., Parman S. W. and Nowell G. M. (2007) A link between large mantle melting events and continent growth seen in osmium isotopes. *Nature* **449**, 202–205.

Petford N. and Atherton M. (1996) Na-rich partial melts from newly underplated basaltic crust: the Cordillera Blanca Batholith. *Peru J. Petrol.* **37**, 1491–1521.

Petford N. and Gallagher K. (2001) Partial melting of mafic (amphibolitic) lower crust by periodic influx of basaltic magma. *Earth Planet. Sci. Lett.* **193**, 483–499.

Pietranik A. B., Hawkesworth C. J., Storey C. D., Kemp A. I. S., Sircombe K. N., Whitehouse M. J. and Bleeker W. (2008) Episodic, mafic crust formation from 4.5 to 2.8 Ga: new evidence from detrital zircons, Slave craton, Canada. *Geology* **36**, 875–878.

Pinet P. and Souriau M. (1988) Continental erosion and large-scale relief. *Tectonics* **7**, 563–582.

Plank T. and Langmuir C. H. (1998) The chemical composition of subducting sediment and its consequences for the crust and mantle. *Chem. Geol.* **145**, 325–394.

Rahl R. M., Reiners P. W., Campbell I. H., Nicolescu S. and Allen C. M. (2003) Combined single-grain (U–Th)/He and U/Pb dating of detrital zircons from the Navajo Sandstone, Utah. *Geology* **31**, 761–764.

Rapp R. P., Shimizu N. and Norman M. D. (2003) Growth of early continental crust by partial melting of eclogite. *Nature* **425**, 605–609.

Rea D. K. and Ruff L. J. (1996) Composition and mass flux of sediment entering the world's subduction zones: implications for global sediment budgets, great earthquakes, and volcanism. *Earth Planet. Sci. Lett.* **140**, 1–12.

Reiners P. W., Spell T. L., Nicolescu S. and Zanetti K. A. (2004) Zircon (U–Th)/He thermochronometry: He diffusion and comparisons with $^{40}Ar/^{39}Ar$ dating. *Geochim. Cosmochim. Acta* **68**, 1857–1887.

Reiners P. W., Campbell I. H., Nicolescu S., Allen C. M., Hourigan J. K., Garver J. I., Mattinson J. M. and Cowan D. S. (2005) (U–Th)/(He–Pb) double dating of detrital zircons. *Am. J. Sci.* **305**, 259–311.

Rey P. F. and Coltice N. (2008) Neoarchean lithospheric strengthening and the coupling of Earth's geochemical reservoirs. *Geology* **36**, 635–638.

Reymer A. and Schubert G. (1984) Phanerozoic addition rates to the continental crust and crustal growth. *Tectonics* **3**, 63–77.

Richards A., Argles T., Harris N., Parrish R., Ahmad T., Darbyshire F. and Draganits E. (2005) Himalayan architecture constrained by isotopic tracers from clastic sediments. *Earth Planet. Sci. Lett.* **236**, 773–796.

Richter F. M. (1988) A major change in the thermal state of the Earth at the Archaean-Proterozoic Boundary: consequences for the nature and preservation of continental lithosphere. *J. Petrol. Spec. Lithosphere Issue*, 39–52.

Rino S., Komiya T., Windley B. F., Katayama I., Motoki A. and Hirata T. (2004) Major episodic increases of continental crustal growth determined from zircon ages of river sands; implications for mantle overturns in the Early Precambrian. *Phys. Earth Planet. Int.* **146**, 369–394.

Rino S., Kon Y., Maruyama S., Santosh M. and Zhao D. (2008) The Grenvillian and Pan-African orogens: World's largest orogenies through geologic time, and their implications on the origin of superplume. *Gondwana Res.* **14**, 51–72.

Roddick J. C. and van Breemen O. (1994) U–Pb dating: a comparison of ion microprobe and single grain conventional analyses. In *Radiogenic Age and Isotope Studies: Report 8; Geological Survey of Canada Current Research 1994-F*, pp. 1–9.

Rogers J. J. W. and Santosh M. (2009) Tectonics and surface effect of the supercontinent Columbia. *Gondwana Res.* **15**, 373–380.

Rollinson H. (2008) Secular evolution of the continental crust: Implications for crust evolution models. *Geochem. Geophys. Geosyst.* **9**, Q12010. doi:10.1029/2008GC002262.

Rubatto D. (2002) Zircon trace element geochemistry: partitioning with garnet and the link between U–Pb ages and metamorphism. *Chem. Geol.* **184**, 123–138.

Rudnick R. L. (1995) Making continental crust. *Nature* **378**, 571–578.

Rudnick R. L. and Fountain D. M. (1995) Nature and composition of the continental crust: a lower crustal perspective. *Rev. Geophys.* **33**, 267–309.

Smithies R. H. (2000) The Archaean tonalite–trondhjemite–granodiorite (TTG) series is not an analogue of Cenozoic adakite. *Earth Planet. Sci. Lett.* **182**, 115–125.

Söderlund U., Patchett P. J., Vervoort J. D. and Isachsen C. E. (2004) The ^{176}Lu decay constant determined by Lu–Hf and U–

Pb isotope systematics of Precambrian mafic intrusions. *Earth Planet. Sci. Lett.* **219**, 311–324.

Stein M. and Golstein S. L. (1996) From plume head to continental lithosphere in the Arabian–Nubian shield. *Nature* **382**, 773–778.

Stein M. and Hofmann A. W. (1994) Mantle plumes and episodic crustal growth. *Nature* **372**, 63–68.

Summerfield M. A. and Hulton N. J. (1994) Natural controls of fluvial denudation rates in major world drainage basins. *J. Geophys. Res.* **99**, 13871–13883.

Tagami T., Galbraith R. F., Yamada G. M. and Laslett G. M. (1998) Revised annealing kinetics of Fission-tracks in zircon and geological implications. In *Advances in Fission-track Geochronology* (eds. P. Van den Haute and F. De Corte). Kluwer Academic Press, pp. 99–112.

Takahashi E. (1990) Speculations on the Archean mantle: missing link between komatiite and depleted garnet peridotite. *J. Geophys. Res.* **95**, 15941–15954.

Tatsumi Y. (2000) Continental crust formation by crustal delamination in subduction zones and complementary accumulation of the enriched mantle I component in the mantle. *Geochem. Geophys. Geosyst.* **1**, 2000GC000094.

Taylor S. R. and McLennan S. M. (1985) The continental crust: its composition and evolution. Blackwell, Oxford.

Thirlwall M. F. and Anczkiewicz R. (2004) Multidynamic isotope ratio analysis using MC-ICP-MS and the causes of secular drift in Hf, Nd and Pb isotope ratios. *Int. J. Mass Spectrom.* **235**, 59–81.

Thorpe R. S., Francis P. W. and Ocallaghan L. (1984) Relative roles of source composition, fractional crystallization and crustal contamination in the petrogenesis of Andean volcanic-rocks. *Philos. Trans. R. Soc. Lond. A* **310**, 675–692.

Tunheng A. and Hirata T. (2004) Development of signal smoothing device for precise elemental analysis using laser ablation-ICP-mass spectrometry. *J. Anal. Atom. Spectrom.* **19**, 932–934.

Ushikubo T., Kita N. T., Cavosie A. J., Wilde S. A., Rudnick R. L. and Valley J. W. (2008) Lithium in Jack Hills zircons: evidence for extensive weathering of Earth's earliest crust. *Earth Planet. Sci. Lett.* **272**, 666–676.

Valley J. W., Lackey J. S., Cavosie A. J., Clechenko C. C., Spicuzza M. J., Basei M. A. S., Bindeman I. N., Ferreira V. P., Sial A. N., King E. M., Peck W. H., Sinha A. K. and Wei C. S. (2005) 4.4 billion years of crustal maturation: oxygen isotope ratios of magmatic zircon. *Contrib. Mineral. Petrol.* **150**, 561–580.

Veevers J. J. (2004) Gondwanaland from 650–500 Ma assembly through 320 Ma merger in Pangea to 185–100 Ma breakup: supercontinental tectonics via stratigraphy and radiometric dating. *Earth Sci. Rev.* **68**, 1–132.

Veevers J. J., Belousova E. A., Saeed A., Sircombe K., Cooper A. F. and Read S. E. (2006) Pan-Gondwana detrital zircons from Australia analysed for Hf-isotopes and trace elements reflect an ice-covered Antarctic provenance of 700–500 Ma age, T^{DM} of 2.0–1.0 Ga, and alkaline affinity. *Earth Sci. Rev.* **76**, 135–174.

Veizer J. and Compston W. (1976) $^{87}Sr/^{86}Sr$ in Precambrian carbonates as an index of crustal evolution. *Geochim. Cosmochim. Acta* **40**, 905–914.

Veizer J. and Jansen S. L. (1979) Basement and sedimentary recycling and continental evolution. *J. Geol.* **87**, 341–370.

Veizer J. and Jansen S. L. (1985) Basement and sedimentary recycling – 2: time dimension to global tectonics. *J. Geol.* **93**, 625–643.

Veizer J. and MacKenzie J. M. (2003) Evolution of sedimentary rocks. In *Sediments Diagenesis, and Sedimentary Rocks*, vol. 7 (ed. J. M. MacKenzie). Elsevier–Pergamon, pp. 369–407.

Velbel M. A. (1999) Bond strength and the relative weathering rates of simple orthosilicates. *Am. J. Sci.* **299**, 679–696.

Vervoort J. D. and Blichert-Toft J. (1999) Evolution of the depleted mantle: Hf isotope evidence from juvenile rocks through time. *Geochim. Cosmochim. Acta* **63**, 533–556.

Vervoort J. D. and Patchett P. J. (1996) Behavior of hafnium and neodymium isotopes in the crust: constraints from Precambrian crustally derived granites. *Geochim. Cosmochim. Acta* **60**, 3717–3733.

Vervoort J. D., Patchett P. J., Blichert-Toft J. and Albarède F. (1999) Relationships between Lu–Hf and Sm–Nd isotopic systems in the global sedimentary system. *Earth Planet. Sci. Lett.* **168**, 79–99.

von Huene R. and Scholl D. W. (1993) The return of sialic material to the mantle indicated by terrigeneous material subducted at convergent margins. *Tectonophysics* **219**, 163–175.

Voshage H., Hofmann A. W., Mazzaucchelli M., Rivalenti G., Sinigoi S., Raczek I. and Demarchi G. (1990) Isotopic evidence from the Ivrea Zone for a hybrid lower crust formed by magmatic underplating. *Nature* **347**, 731–736.

Wang C. Y., Campbell I. H., Allen C. M., Williams I. S. and Eggins S. M. (2009) Rate of growth of the preserved North American continental crust: evidence from Hf and O isotopes in Mississippi detrital zircons. *Geochim. Cosmochim. Acta* **73**, 712–728.

Watson E. B. and Harrison T. M. (2005) Zircon thermometer reveals minimum melting conditions on earliest Earth. *Science* **308**, 841–844.

Wedepohl K. H. (1995) The composition of the continental crust. *Geochim. Cosmochim. Acta* **59**, 1217–1232.

Whalen J. B., Percival J. A., McNicoll V. J. and Longstaffe F. J. (2002) A mainly crustal origin for tonalitic granitoid rocks, Superior Province, Canada: implications for late Archean tectonomagmatic processes. *J. Petrol.* **43**, 1551–1570.

Wiedenbeck M., Alle P., Corfu F., Griffin W. L., Meier M., Ober F., Von Quant A., Roddick J. C. and Spiegel J. (1995) Three natural zircon standards for U–Th–Pb, Lu–Hf, trace element and REE analyses. *Geostand. Newslett.* **19**, 1–23.

Windley B. F. (1995) The Evolving Continents. *third ed.*. Wiley, New York.

Woodhead J. D. and Hergt J. M. (2005) A preliminary appraisal of seven natural zircon reference materials for in situ Hf isotope determination. *Geostand. Geoanal. Res.* **29**, 183–195.

Woodhead J., Hergt J., Shelley M., Eggins S. and Kemp R. (2004) Zircon Hf-isotope analysis with an excimer laser, depth profiling, ablation of complex geometries, and concomitant age estimation. *Chem. Geol.* **209**, 121–135.

Wu F. Y., Yang Y. H., Xie L. W., Yang J. H. and Xu P. (2006) Hf isotopic compositions of the standard zircons and baddeleyites used in U–Pb geochronology. *Chem. Geol.* **234**, 105–126.

Wyllie P. J. (1984) Constraints imposed by experimental petrology on possible and impossible magma sources and products. *Philos. Trans. R. Soc. Lond. A* **310**, 439–456.

Yang J., Gao S., Chen C., Tang Y. Y., Yuan H. L., Gong H. J., Xie S. W. and Wang J. Q. (2009) Episodic crustal growth of North China as revealed by U–Pb age and Hf isotopes of detrital zircons from modern rivers. *Geochim. Cosmochim. Acta* **73**, 2660–2673.

Zhao G., Sun M., Wilde S. A. and Li S. (2004) A Paleo–Mesoproterozoic supercontinent: assembly, growth and breakup. *Earth Sci. Rev.* **67**, 91–123.

Associate editor: Alan D. Brandon